

SUPPORTING INFORMATION

Synthesis, Binding and Antiviral Properties of Potent Core-Extended Naphthalene Diimide Targeting the HIV-1 Long Terminal Repeat Promoter G-quadruplexes

Rosalba Perrone,^{†,§} Filippo Doria,^{‡,§} Elena Butovskaya,^{†,§} Ilaria Frasson,[†] Silvia Botti,[‡] Matteo Scalabrin,[†] Sara Lago,[†] Vincenzo Grande,[‡] Matteo Nadai,[†] Mauro Freccero,^{*,‡} and Sara N. Richter^{*,†}

[†]Department of Molecular Medicine, University of Padua, via Gabelli 63, 35121 Padua, Italy

[‡]Department of Chemistry, University of Pavia, V.le Taramelli 10, 27100 Pavia, Italy

Table of content

Table S1. List of oligonucleotides used in this study.	S2
Table S2. C-exNDIs ΔT_m values obtained in the FRET melting assay.	S3
Table S3. Cartesian coordinates of a prototype c-exNDI	S4-S5
Figure S1. Size comparison between a) the NDI and b) c-exNDI cores	S6
Figure S2: CD analysis of LTR-III, LTR-IV and hTel G4 oligonucleotides in the absence/presence of 2 .	S7-S9
Figure S3. CD analysis of G4-folded oligonucleotides in MS buffer conditions.	S10
Figure S4. ESI/MS competition analysis.	S11
Figure S5. ESI/MS analysis of 2 binding stoichiometry to LTR-III G4.	S12
Figure S6. SPR analysis of 2 binding affinity to LTR-IV and hTel G4s.	S13
Figure S7. Assessment of 2 cell entry by microscopy.	S14
HPLC PURITY DATA	S15-S1
¹ H- and ¹³ C-NMR spectra of the compounds 1 , 5 , 6 and 7	S20-S29

Table S1. Oligonucleotides used in this study

Application	Name	Sequence 5'-3'
FRET assay	LTR-III	<i>FAM</i> -TGGGAGGCGTGGCCTGGGCGGGACTGGGGT- <i>TAMRA</i>
	LTR-IV	<i>FAM</i> -TGGGCGGGACTGGGGAGTGGT- <i>TAMRA</i>
	F21T	<i>FAM</i> -GGGTTAGGGTTAGGGTTAGGG- <i>TAMRA</i>
	dsDNA	<i>FAM</i> -CTATAGCGCGCTATAG- <i>TAMRA</i>
CD and MS assays	LTR-III	GGGAGGCGTGGCCTGGGCGGGACTGGGG
	LTRIV	TGGGCGGGACTGGGGAGTGGT
	hTel	GGGTTAGGGTTAGGGTTAGGG
	c-kit2	CGGGCGGGCGCGAGGGAGGGG
	c-myc	TGGGGAGGGTGGGGAGGGTGGGGGAAGG
<i>Taq</i> polymerase stop assay	<i>Taq</i> Primer	GGCAAAAAGCAGCTGCTTATATGCAG
	No G4	TTGTCGTTAAAGTCTGACTGCGAGCTCTCAGATCCTGCAT ATAAGCAGCTGCTTTTTGCC
	hTel	TTTTTGGGTTAGGGTTAGGGTTAGGGTTTTTCTGCATATA AGCAGCTGCTTTTTGCC
	LTR III	TTTTTGGGAGGCGTGGCCTGGGCGGGACTGGGGAGTGGT TTTTTCTGCATATAAGCAGCTGCTTTTTGCC
	LTR IV	TTTTTGGGCGGGACTGGGGAGTGGTTTTTCTGCATATAAG CAGCTGCTTTTTGCC

FAM: 6-carboxyfluorescein, *TAMRA*: 6-carboxy-tetramethylrhodamine

Table S2. C-exNDIs ΔT_m values obtained in the FRET melting assay. Equimolar amounts of the compounds were added to each FAM (6-carboxyfluorescein) 5'-end- and TAMRA (6-carboxy-tetramethylrhodamine) 3'-end-labelled oligonucleotide (0.25 μ M) folded in the lithium cacodylate buffer supplemented with potassium (100 mM).

c-exNDIs	LTR-III	LTR-IV	hTel	dsDNA
2	10.5 \pm 0.1	11.7 \pm 0.6	6.0 \pm 0.1	1.5 \pm 0.1
3	7.0 \pm 0.7	10.3 \pm 1.1	3.5 \pm 0.7	1.6 \pm 0.4
4	7.0 \pm 0.7	12.0 \pm 1.7	5.3 \pm 1.1	1.6 \pm 0.5
5	2.5 \pm 0.1	5.0 \pm 0.1	2.0 \pm 0.1	1.1 \pm 0.6
6	5.0 \pm 0.7	6.3 \pm 0.6	4.2 \pm 0.3	1.8 \pm 0.6
7	3.7 \pm 1.0	4.7 \pm 0.6	3.0 \pm 0.1	1.5 \pm 0.1
8	1.5 \pm 0.1	3.0 \pm 0.1	1.5 \pm 0.7	1.1 \pm 0.6
9	1.2 \pm 1.1	3.0 \pm 1.0	0.5 \pm 0.7	0.5 \pm 0.1
10	12.4 \pm 0.1	16.0 \pm 1.7	8.5 \pm 0.6	4.1 \pm 0.6
11	5.5 \pm 0.1	11.7 \pm 1.2	3.8 \pm 0.3	1.5 \pm 0.6

Table S2. Cartesian coordinates of the **c-exNDI** core (Scheme 1, R₂=CH₃, R₃=Y=H) optimised at B3LYP/6-31+G(d,p) level of theory, in gas phase, using Gaussian 09, Revision B.01 software package.

Center Number	Atomic Number	Atomic Type	Coordinates (Angstroms)		
			X	Y	Z
1	6	0	-0.217963	-2.890097	-0.000065
2	6	0	-0.210573	-1.429193	-0.000147
3	6	0	-1.450603	-0.710875	-0.000178
4	6	0	-2.679294	-1.396967	-0.000121
5	6	0	-2.701691	-2.872757	-0.000130
6	6	0	1.002582	-0.725637	-0.000164
7	6	0	-1.450606	0.710875	-0.000252
8	6	0	-0.210578	1.429200	-0.000288
9	6	0	1.002583	0.725650	-0.000206
10	6	0	-0.217978	2.890104	-0.000228
11	6	0	-2.701709	2.872749	-0.000221
12	6	0	-2.679301	1.396959	-0.000203
13	6	0	-3.893181	0.694469	-0.000050
14	6	0	-3.893178	-0.694485	-0.000060
15	1	0	-4.818044	1.260047	0.000021
16	8	0	-3.735670	3.532525	0.000780
17	8	0	0.829008	3.567832	0.000517
18	8	0	-3.735646	-3.532542	-0.000082
19	8	0	0.829030	-3.567819	-0.000101
20	7	0	-1.458036	-3.528911	0.000183
21	7	0	-1.458059	3.528909	-0.000463
22	6	0	-1.503535	-4.998420	0.000408
23	6	0	-1.503570	4.998420	-0.000160
24	1	0	-2.044109	5.346589	-0.882700
25	1	0	-0.481647	5.367348	-0.004398
26	1	0	-2.042154	-5.346457	0.884197
27	1	0	-0.481601	-5.367338	0.002629
28	1	0	-2.036402	5.346903	0.887019
29	1	0	-2.038288	-5.347048	-0.885535
30	1	0	2.141728	-2.381023	0.000014
31	1	0	2.141735	2.381033	-0.000273
32	6	0	3.440486	0.703687	-0.000125
33	6	0	3.440486	-0.703676	-0.000075
34	6	0	4.650709	1.403085	-0.000087
35	1	0	4.639964	2.489027	-0.000115
36	6	0	4.650706	-1.403079	-0.000011
37	1	0	4.639958	-2.489020	-0.000004
38	6	0	5.856171	-0.699850	0.000007
39	1	0	6.794033	-1.245446	0.000026
40	6	0	5.856173	0.699852	-0.000019
41	1	0	6.794035	1.245449	0.000036
42	1	0	-4.818040	-1.260064	-0.000019
43	7	0	2.211187	-1.356421	-0.000088
44	7	0	2.211189	1.356433	-0.000195

Gaussian 09, Revision B.01, M. J. Frisch, G. W. Trucks, H. B. Schlegel, G. E. Scuseria, M. A. Robb, J. R. Cheeseman, G. Scalmani, V. Barone, B. Mennucci, G. A. Petersson, H. Nakatsuji, M. Caricato, X. Li, H. P. Hratchian, A. F. Izmaylov, J. Bloino, G. Zheng, J. L. Sonnenberg, M. Hada, M. Ehara, K. Toyota, R. Fukuda, J. Hasegawa, M. Ishida, T. Nakajima, Y. Honda, O. Kitao, H. Nakai, T. Vreven, J. A. Montgomery, Jr., J. E. Peralta, F. Ogliaro, M. Bearpark, J. J. Heyd, E. Brothers, K. N. Kudin, V. N. Staroverov, T. Keith, R. Kobayashi, J. Normand, K. Raghavachari, A.

Rendell, J. C. Burant, S. S. Iyengar, J. Tomasi, M. Cossi, N. Rega, J. M. Millam, M. Klene, J. E. Knox, J. B. Cross, V. Bakken, C. Adamo, J. Jaramillo, R. Gomperts, R. E. Stratmann, O. Yazyev, A. J. Austin, R. Cammi, C. Pomelli, J. W. Ochterski, R. L. Martin, K. Morokuma, V. G. Zakrzewski, G. A. Voth, P. Salvador, J. J. Dannenberg, S. Dapprich, A. D. Daniels, O. Farkas, J. B. Foresman, J. V. Ortiz, J. Cioslowski, and D. J. Fox, Gaussian, Inc., Wallingford CT, 2010.

Figure S1. Size comparison between a) the **NDI** and b) **c-exNDI** cores. The size of the NDI, as well as the G4 size [reported in c) and d)], have been evaluated from the crystal structure of the intramolecular human telomeric DNA G-quadruplex bound by the di-substituted NDI BMSG-SH-3 (3SC8.pdb, from Reference: Collie, G.W., Promontorio, R., Hampel, S.M., Micco, M., Neidle, S., Parkinson, G.N. Structural basis for telomeric G-quadruplex targeting by naphthalene diimide ligands. *J. Am. Chem. Soc.* **2012**, *134*, 2723-2731). The size of the **c-exNDI** core was evaluated from DFT calculations in gas phase, at B3LYP/6-31+G(d,p) level of theory. Overlap of the c) **NDI** and d) **c-exNDI** cores to the intramolecular human telomeric DNA G-quartet, for an estimation of the ligand-quartet overlap extension.

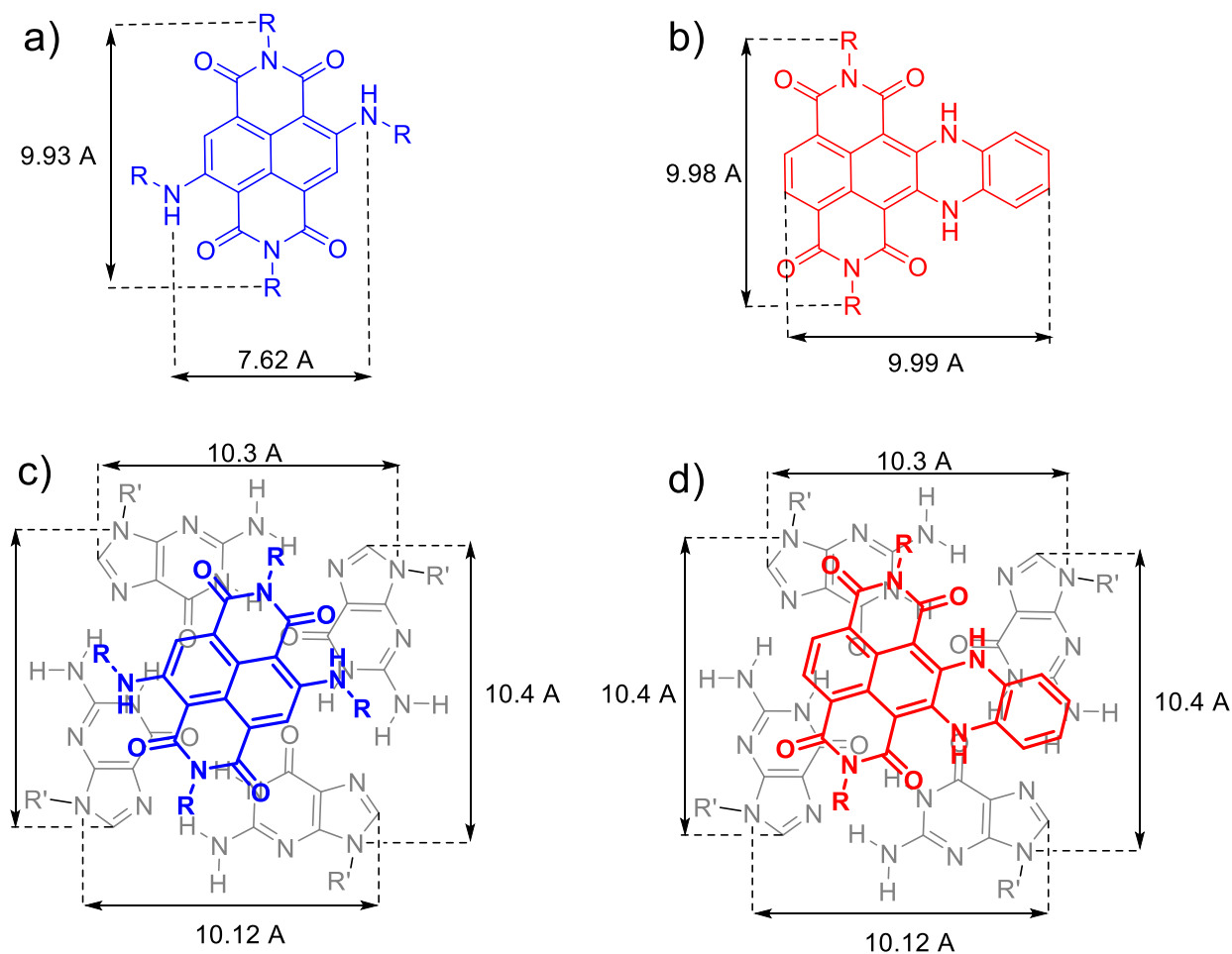
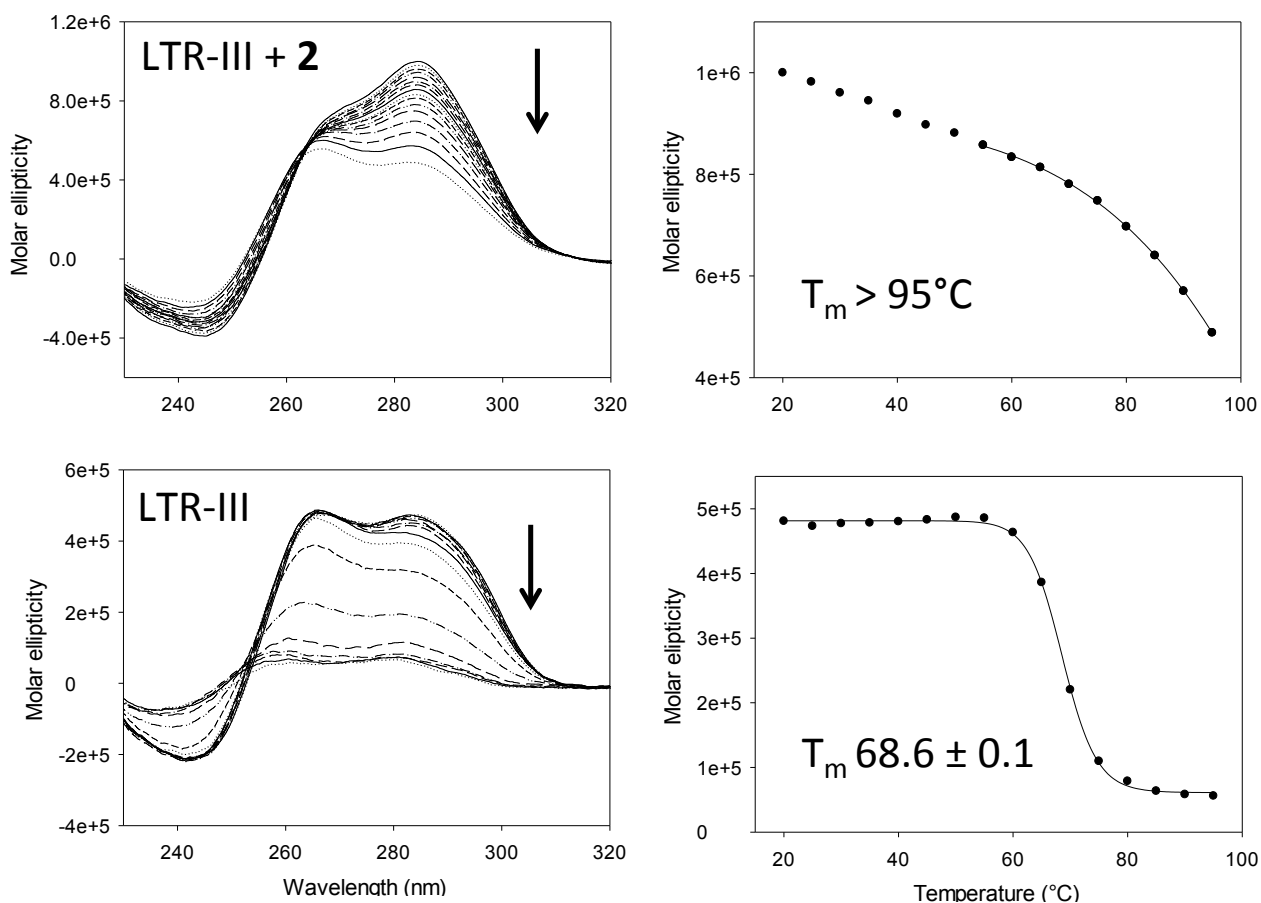
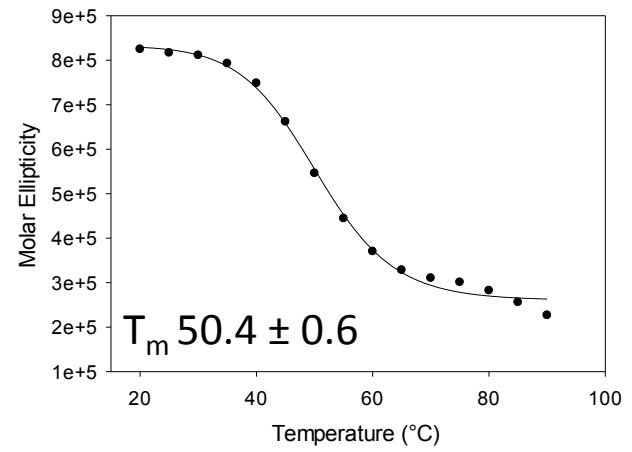
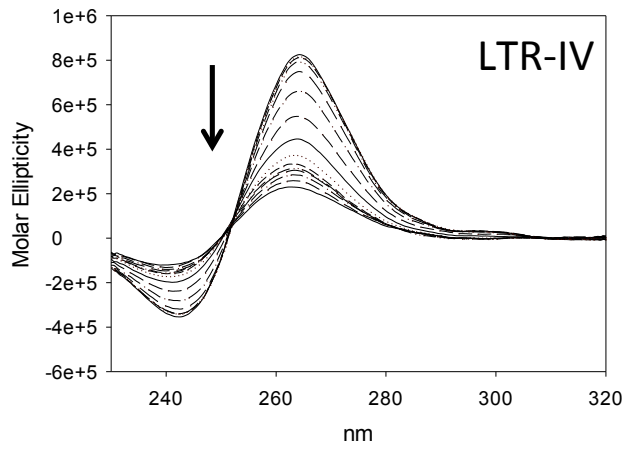
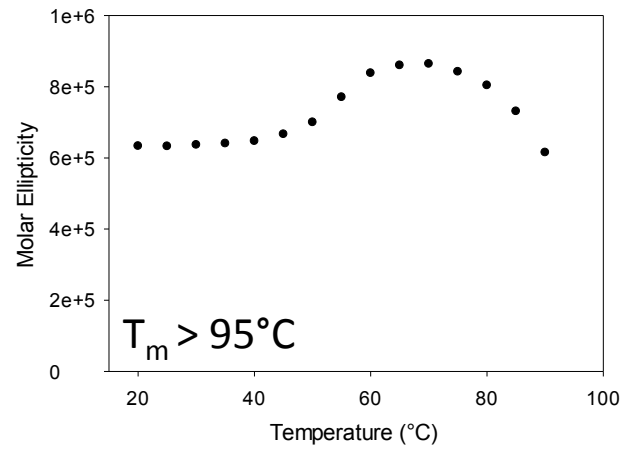
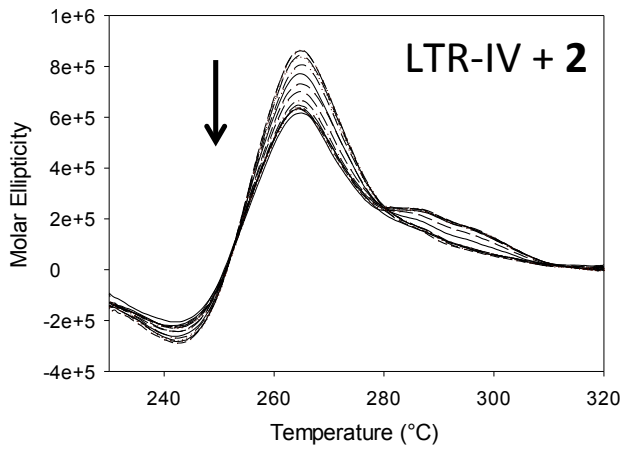


Figure S2. CD analysis of LTR-III (A), LTR-IV (B) and hTel (C) G4 oligonucleotides in the absence (lower panels) and in the presence of compound **2** (upper panels). The left panels show CD spectra variation in function of the temperature; arrows indicate the spectral change from low to high temperatures. The right panels show the molar ellipticity at the peak wavelength as a function of the temperature.

A



B

C

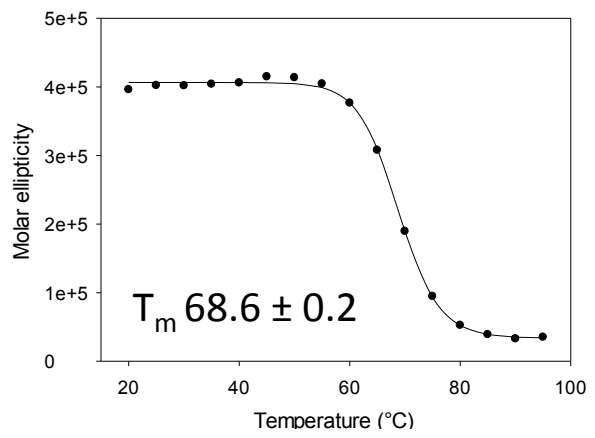
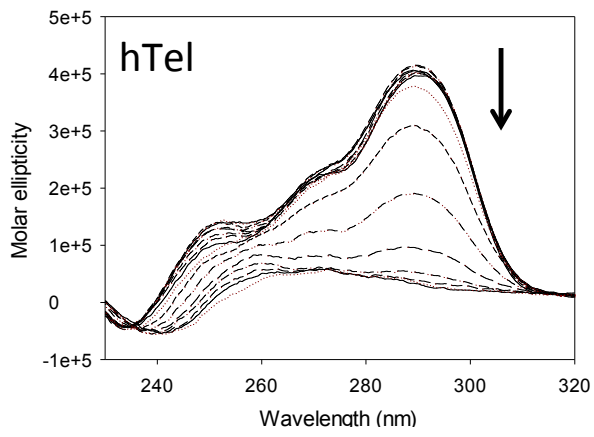
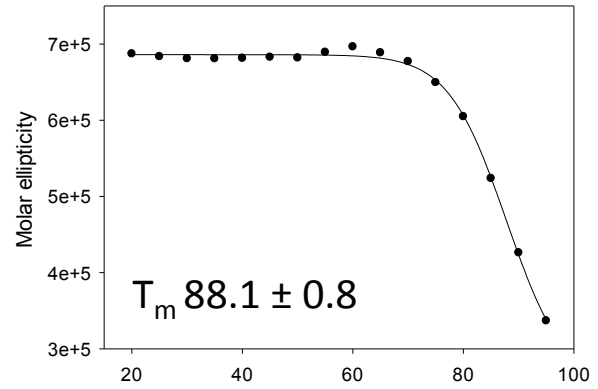
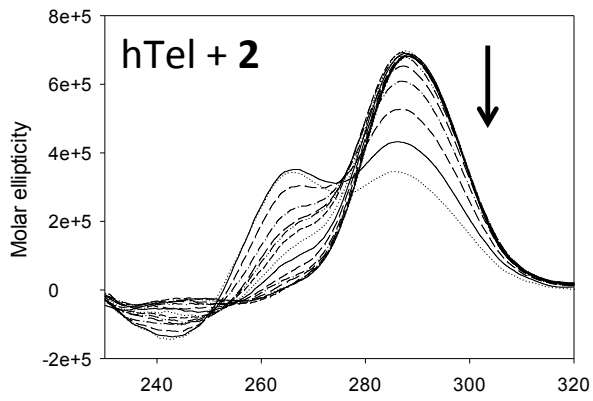


Figure S3. CD analysis of G4-folded oligonucleotides in MS buffer conditions.

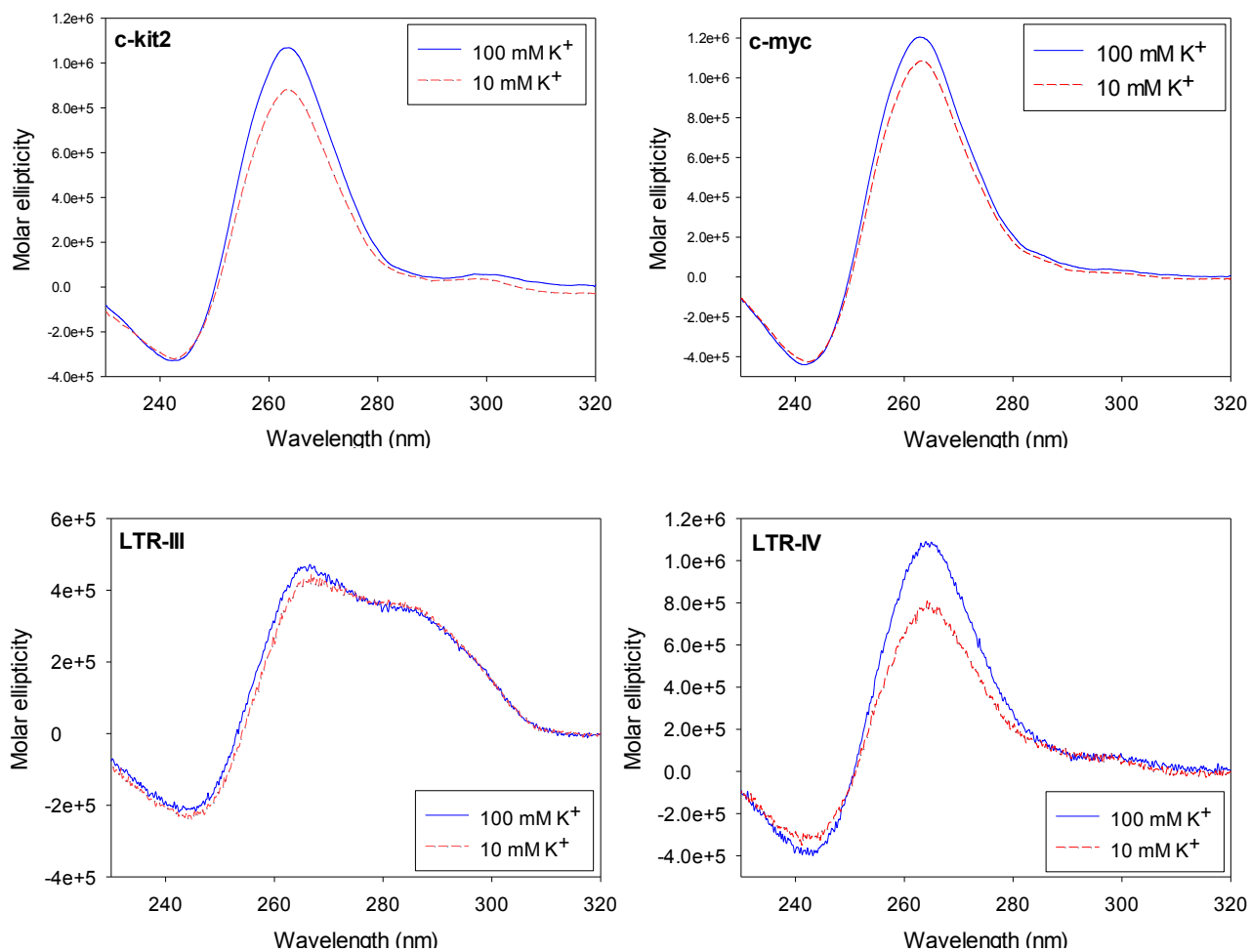


Figure S4. ESI/MS competition analysis. Equimolar amounts of LTR-III/hTel (A), LTR-IV/hTel (B), LTR-III/LTR-IV (C) were incubated with 2-fold excess of **2** (left panels) or **4** (right panels) and analysed by ESI/MS. The identity of m/z signals is shown above each signal. RI stands for relative intensity.

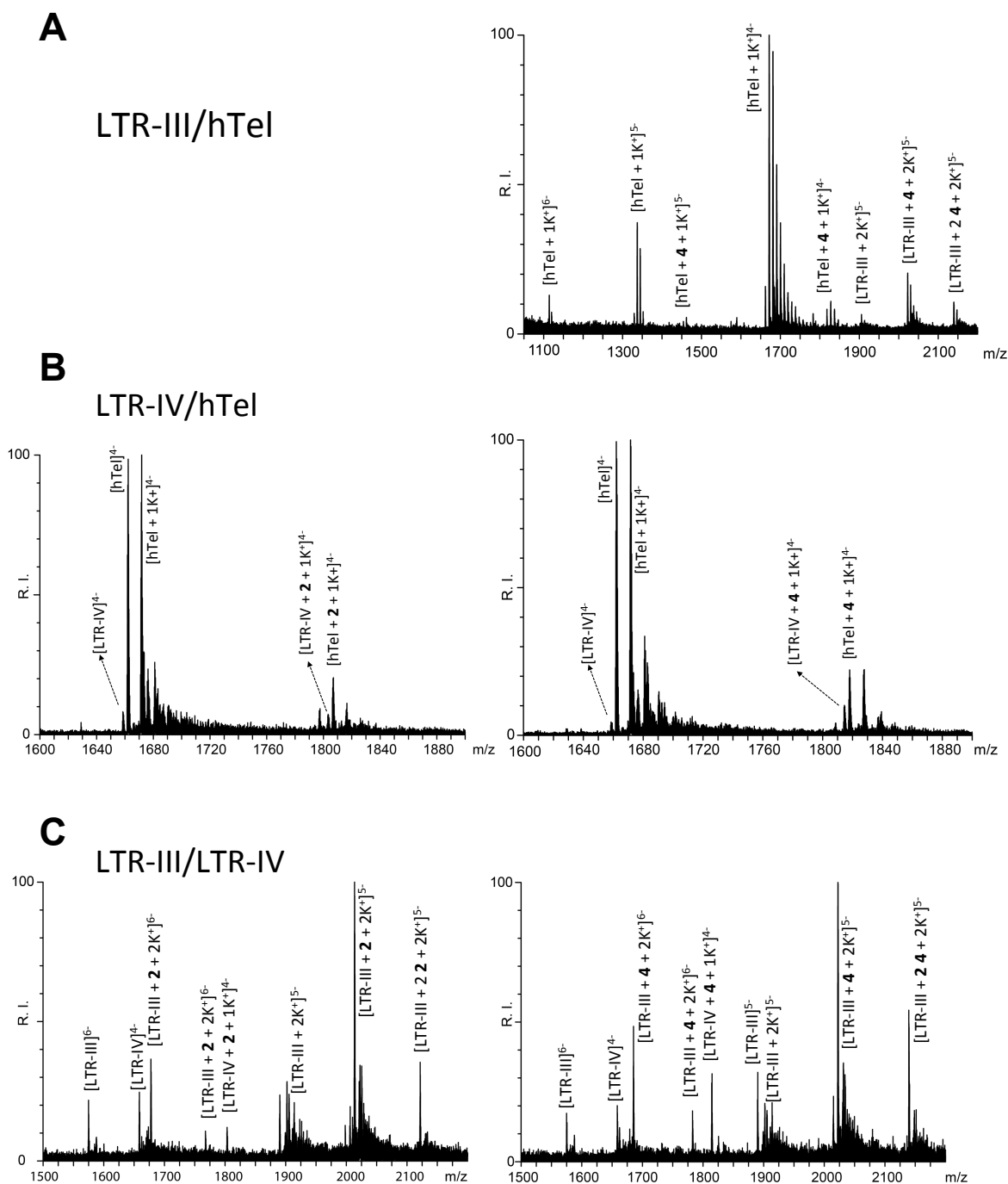


Figure S5. ESI/MS analysis of **c-exNDI 2** binding stoichiometry at saturating concentration (10-fold molar excess) towards the G4 structures. Representative spectrum of **c-exNDI 2** and LTR-III G4.

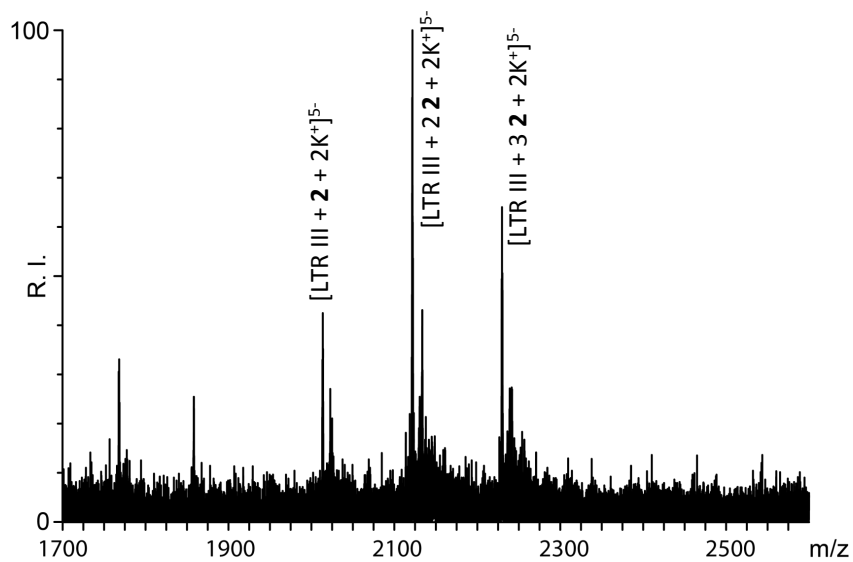


Figure S6. SPR analysis of **2** binding towards LTR-IV (upper panel) and hTel (lower panel) G4s. Biosensor data were collected at 25°C; the compound was injected at increasing concentrations (50, 100, 200, 300 nM). Sensograms are shown as grey lines. Dotted black lines represent local 1:1 binding fits obtained for a calculated R_{\max} of 33.6 (LTR-IV) and 34.8 (hTel) RU (Response Units).

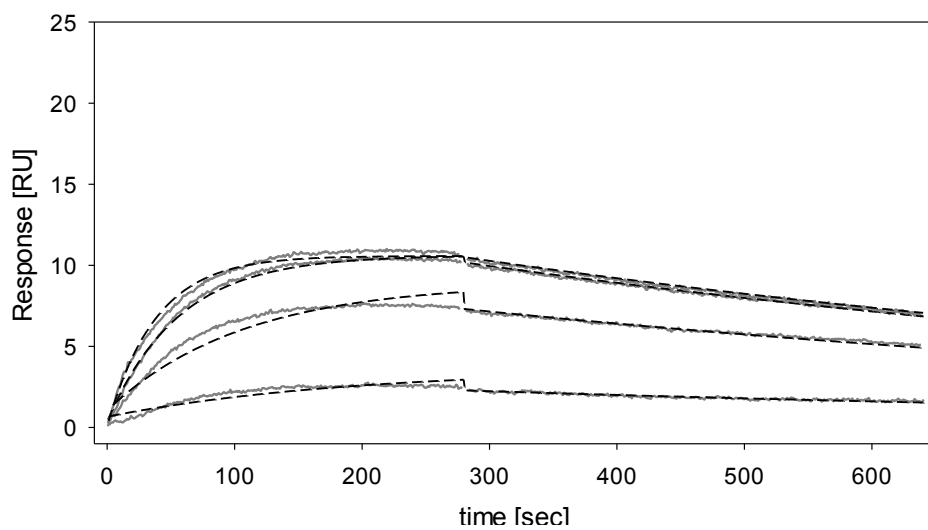
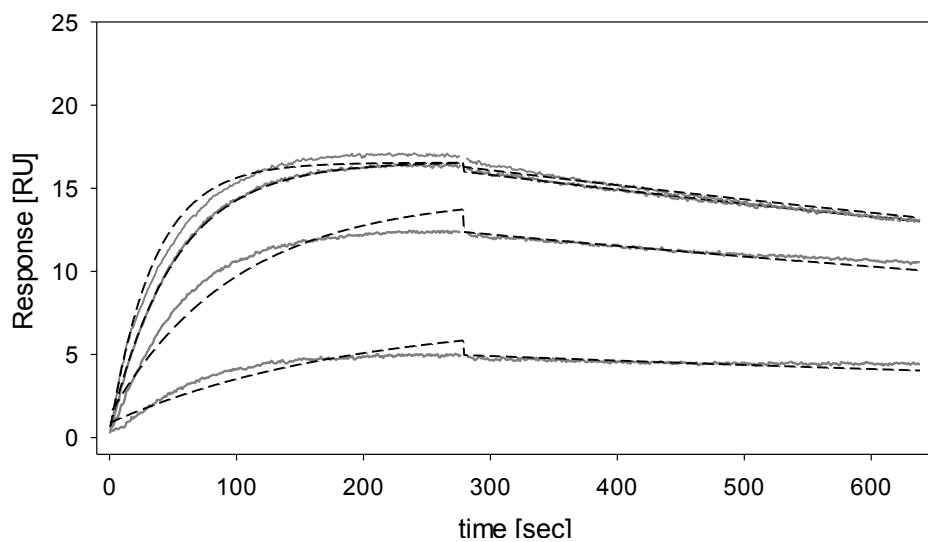
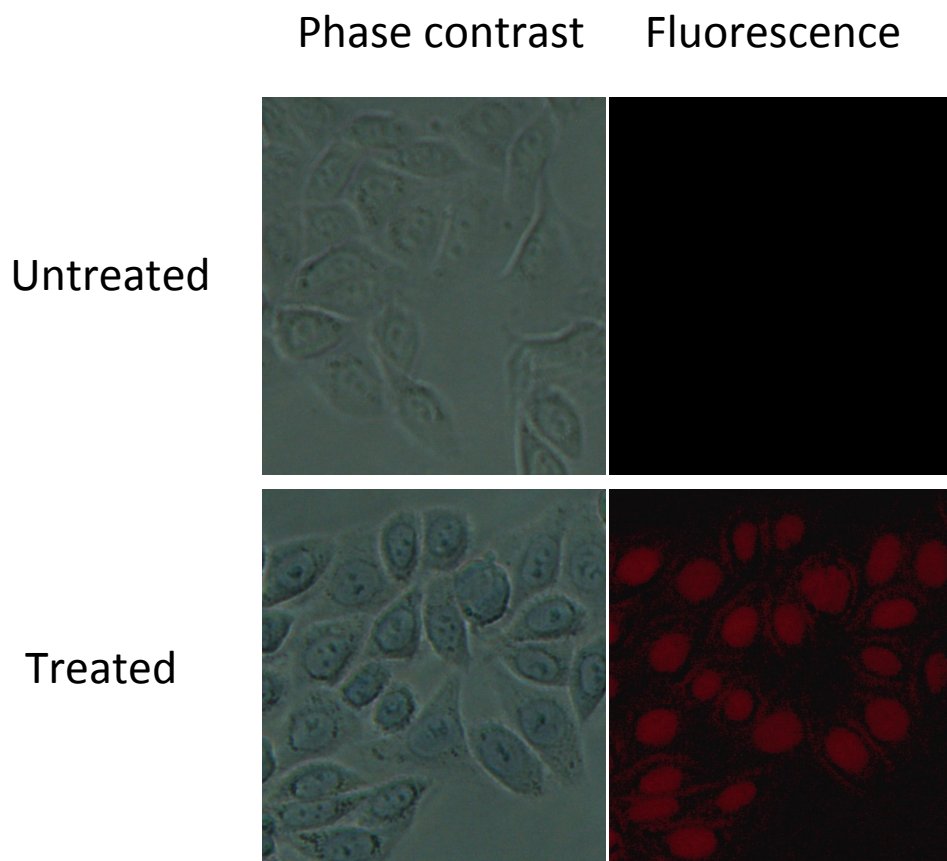
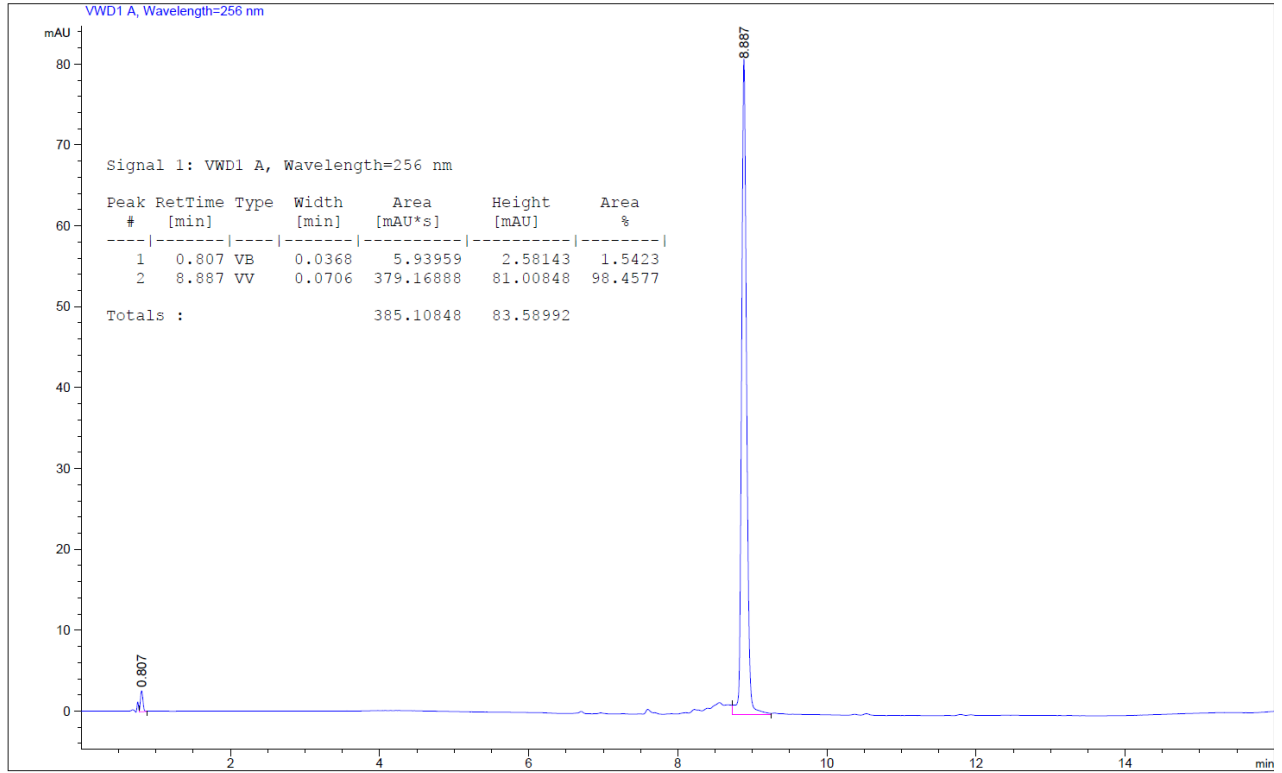


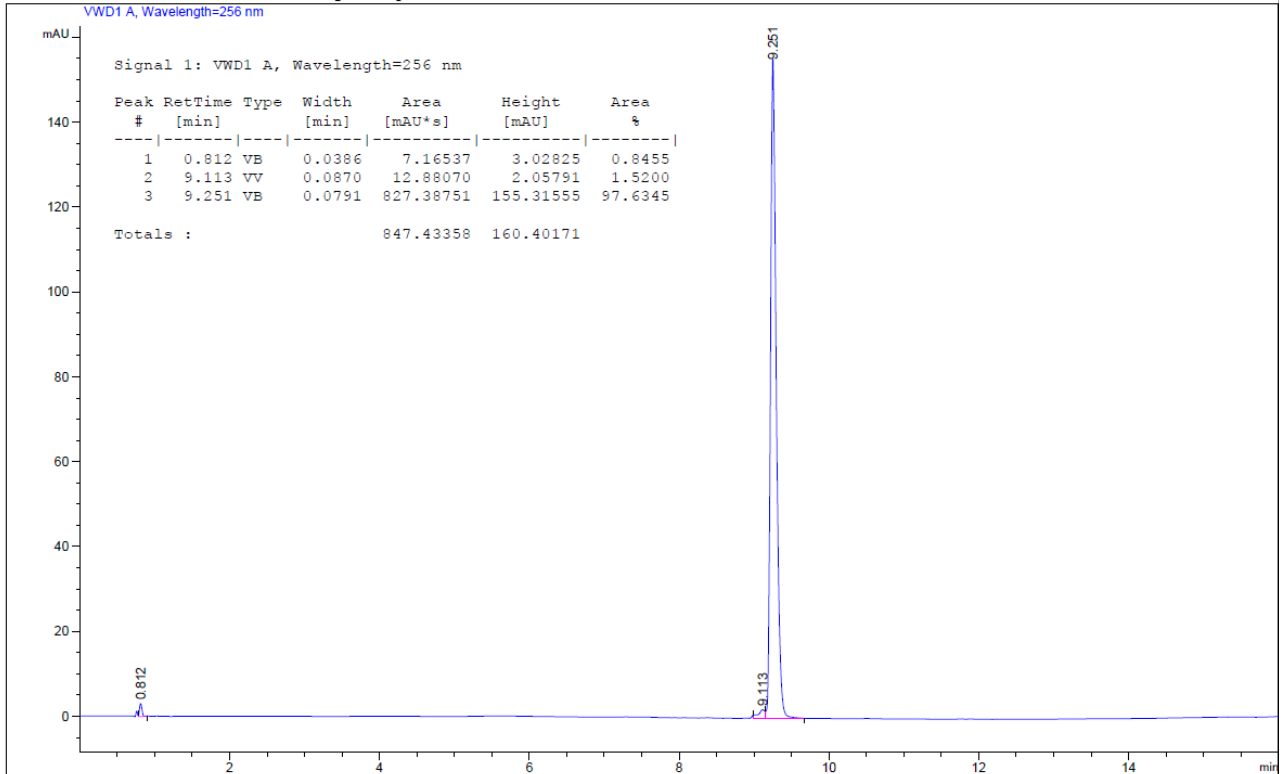
Figure S7. Assessment of **2** cell entry by fluorescence microscopy. TZM-bl cells were seeded (15000 cells/well) in μ Clear black 96 well plate (CELLSTAR®, Greiner Bio-One GmbH, Frickenhausen, Germany) and treated with **2** ($12.5 \mu\text{M}$). After 30 min, the medium was replaced with PBS 1X and cells were observed with the fluorescence microscope Leica DFC 420C (Leica Microsystems Srl, Milano, Italy) equipped with a mercury AC lamp (Leistungselektronik JENA GmbH, Jena, Germany) and an appropriate filter to visualize the red fluorescence of the compound with a 20X ocular objective. Images were acquired with Leica Application Suite V3.8 program (Leica Microsystems Srl, Milano, Italy).



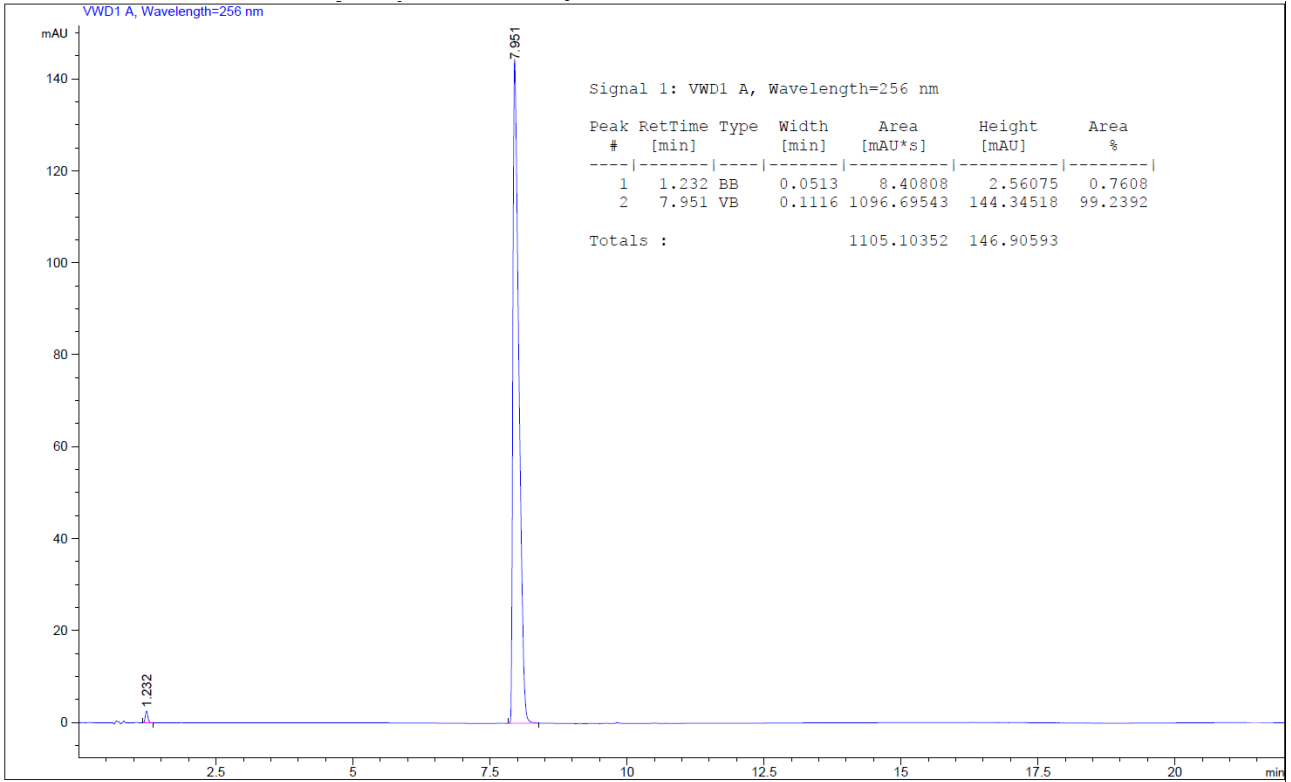
4·2HCl
Analytical Method-A



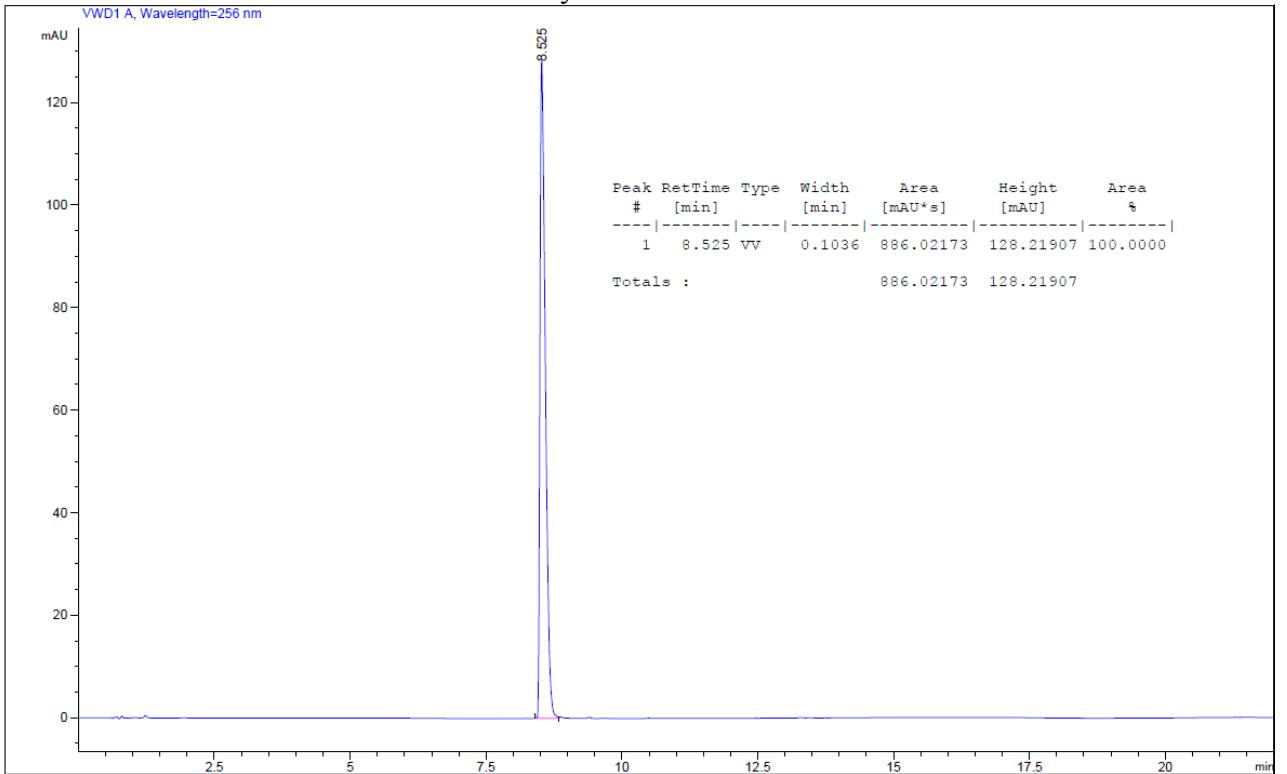
5·2HCl
Analytical Method-A



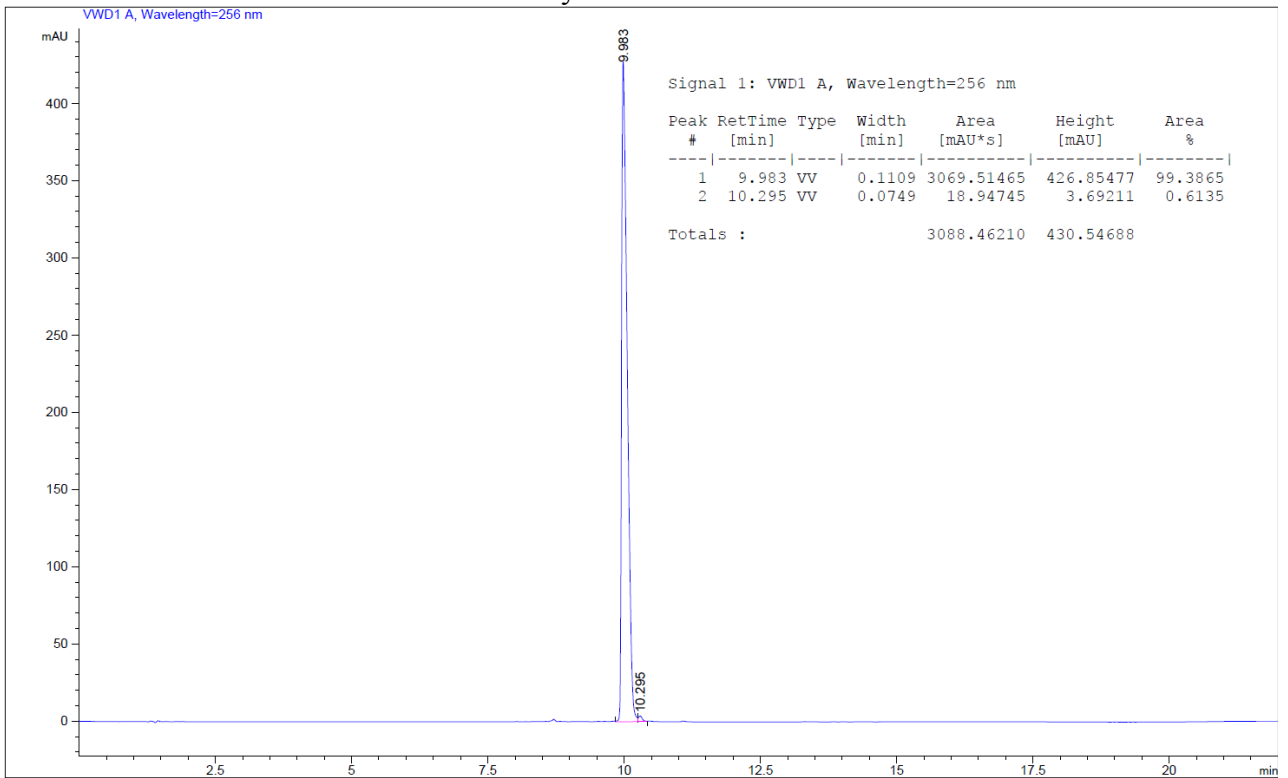
6·2HCl
Analytical Method-A



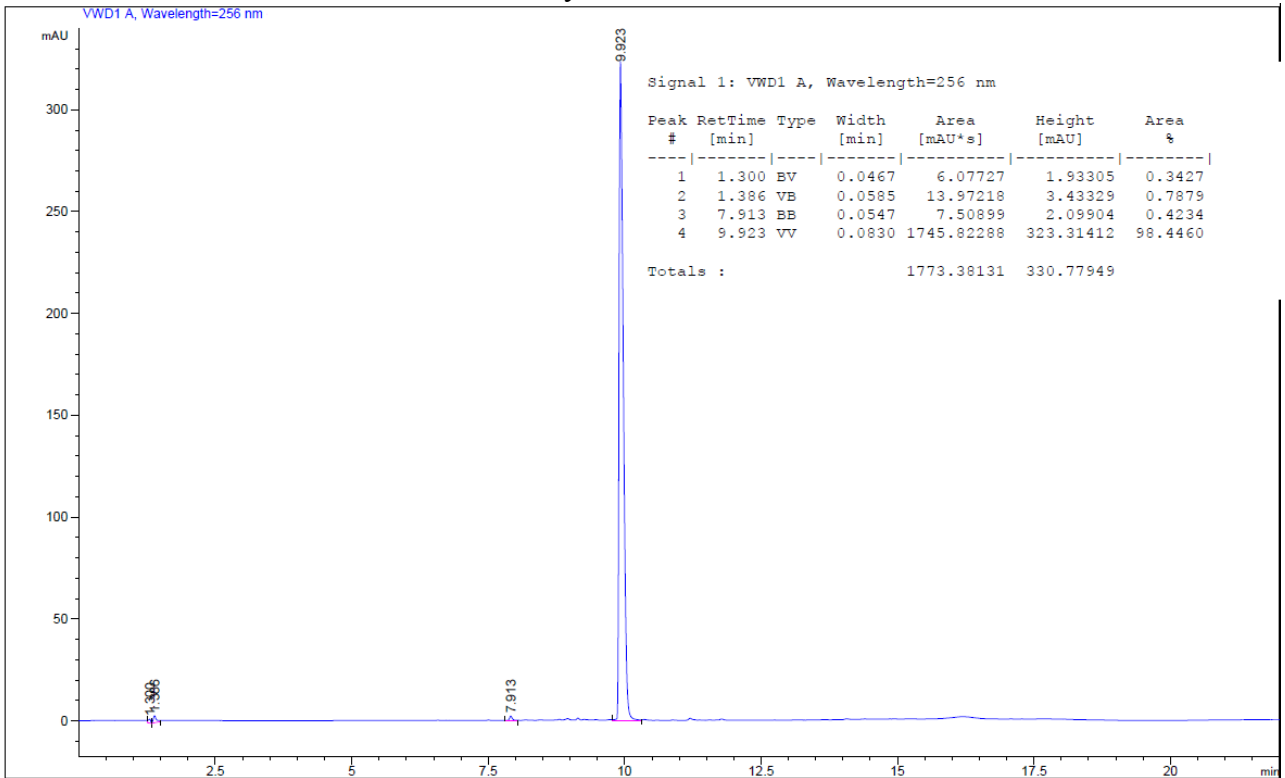
7·2HCl
Analytical Method-A



8·2HCl Analytical Method-A

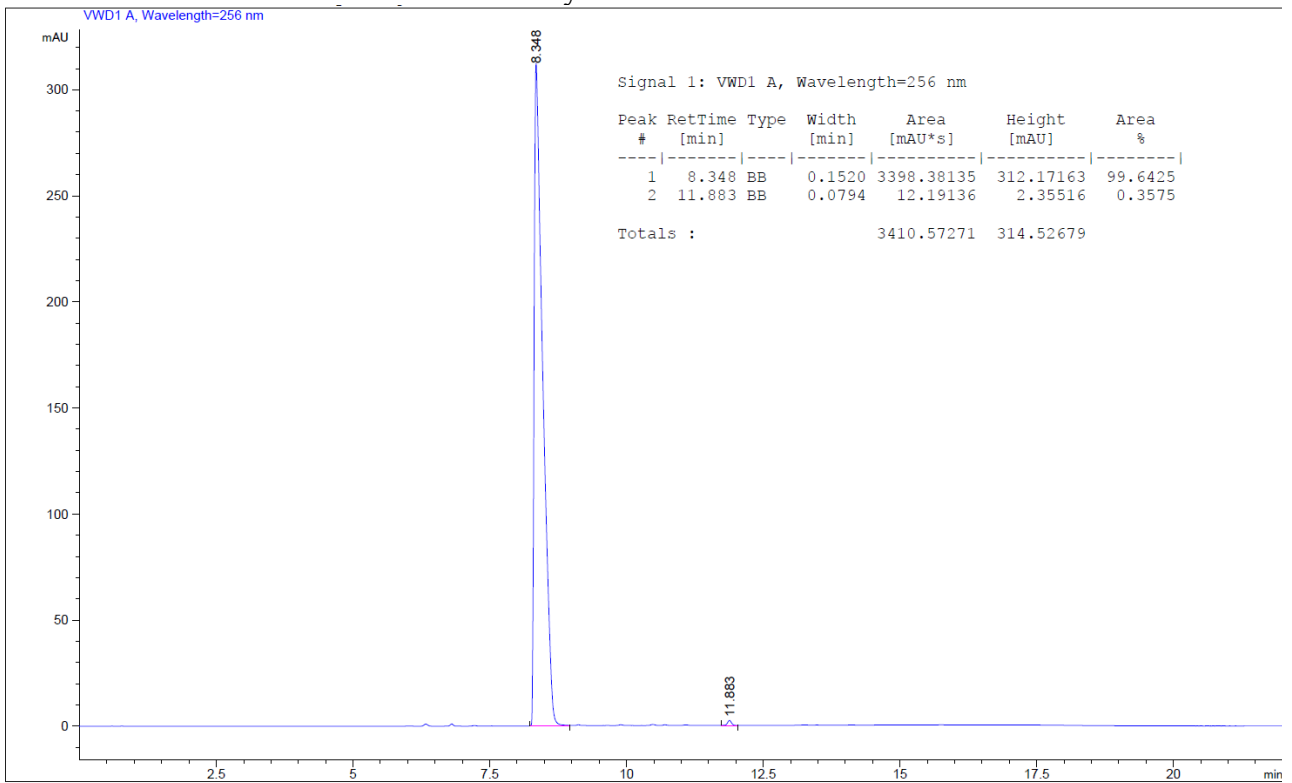


9·3HCl Analytical Method-A



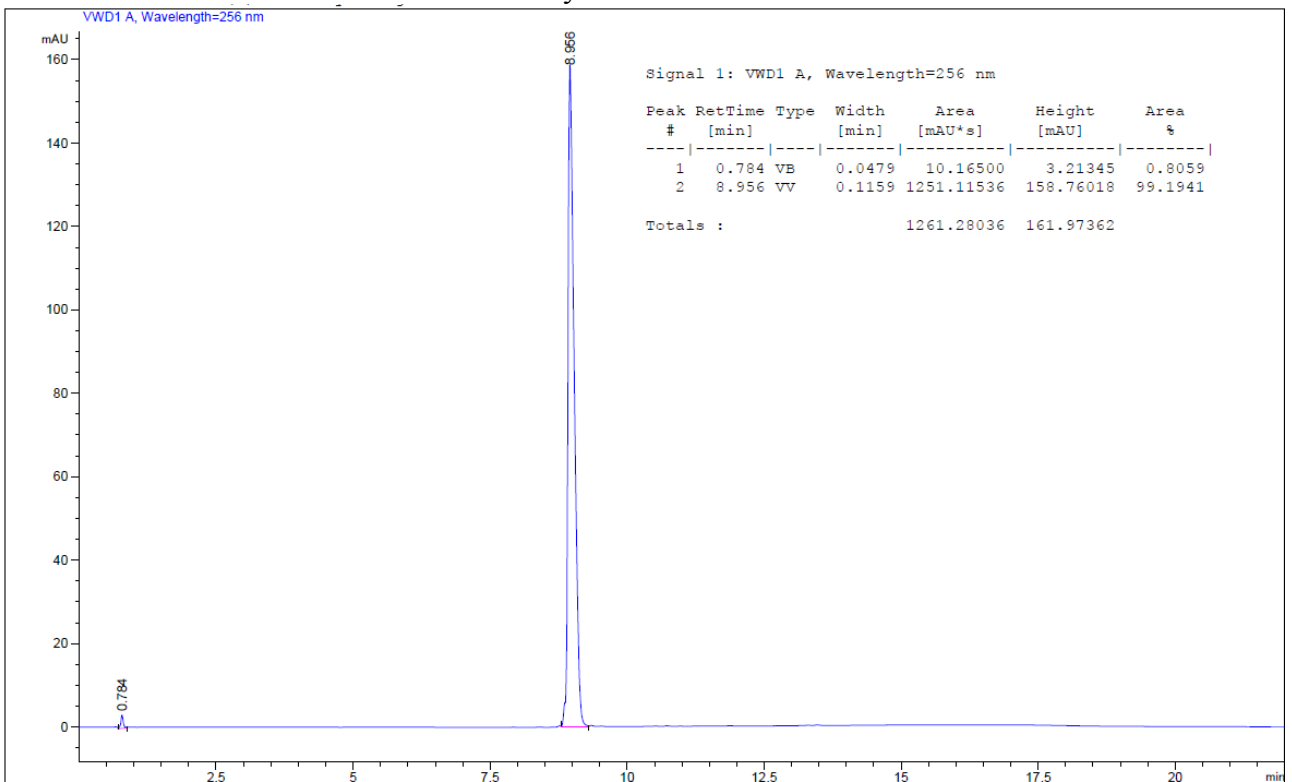
10

Analytical Method-A



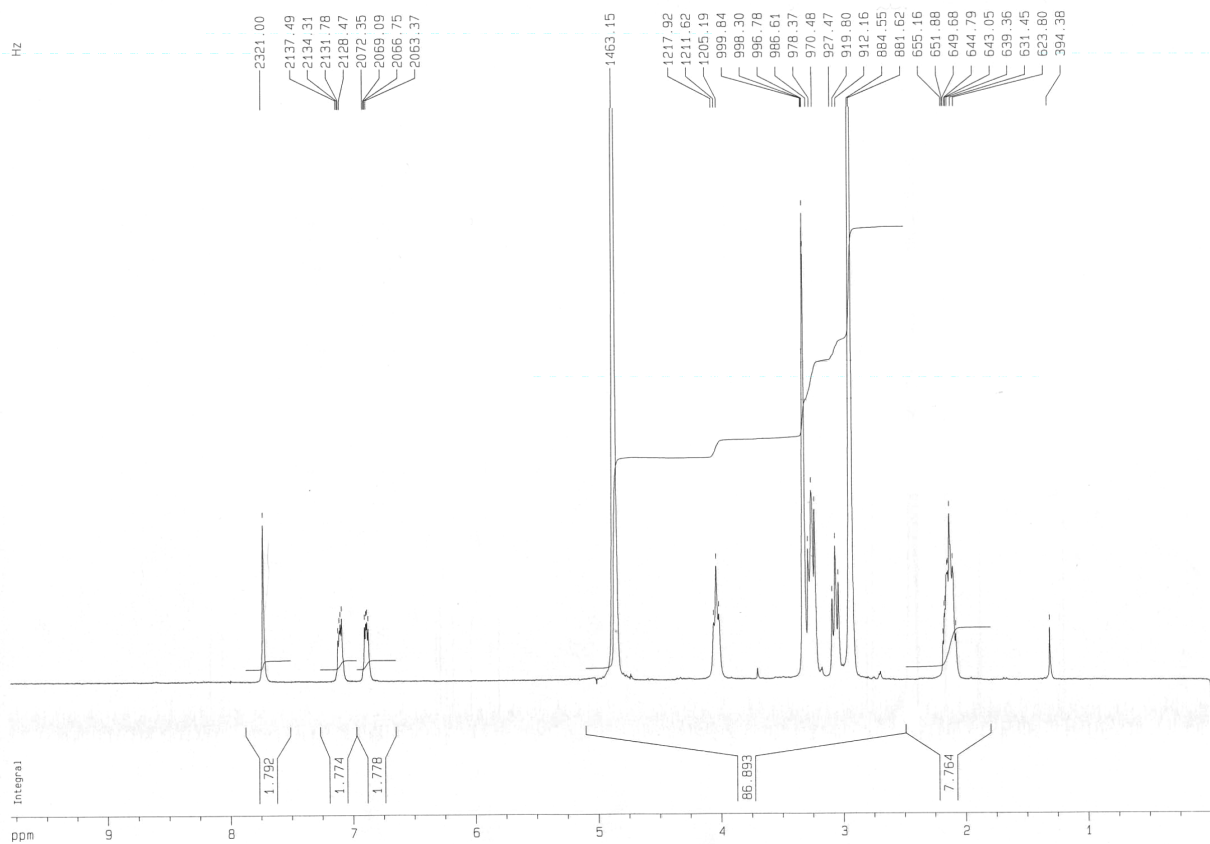
11

Analytical Method-A

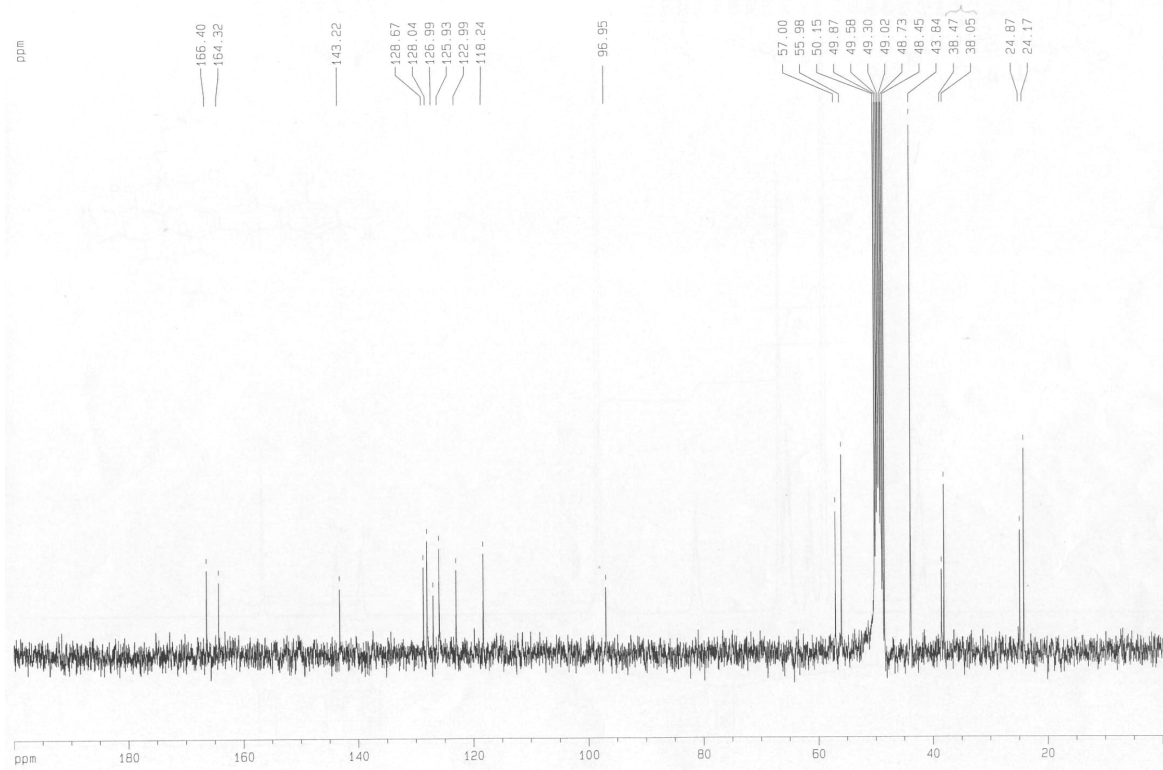


NMR Spectra:

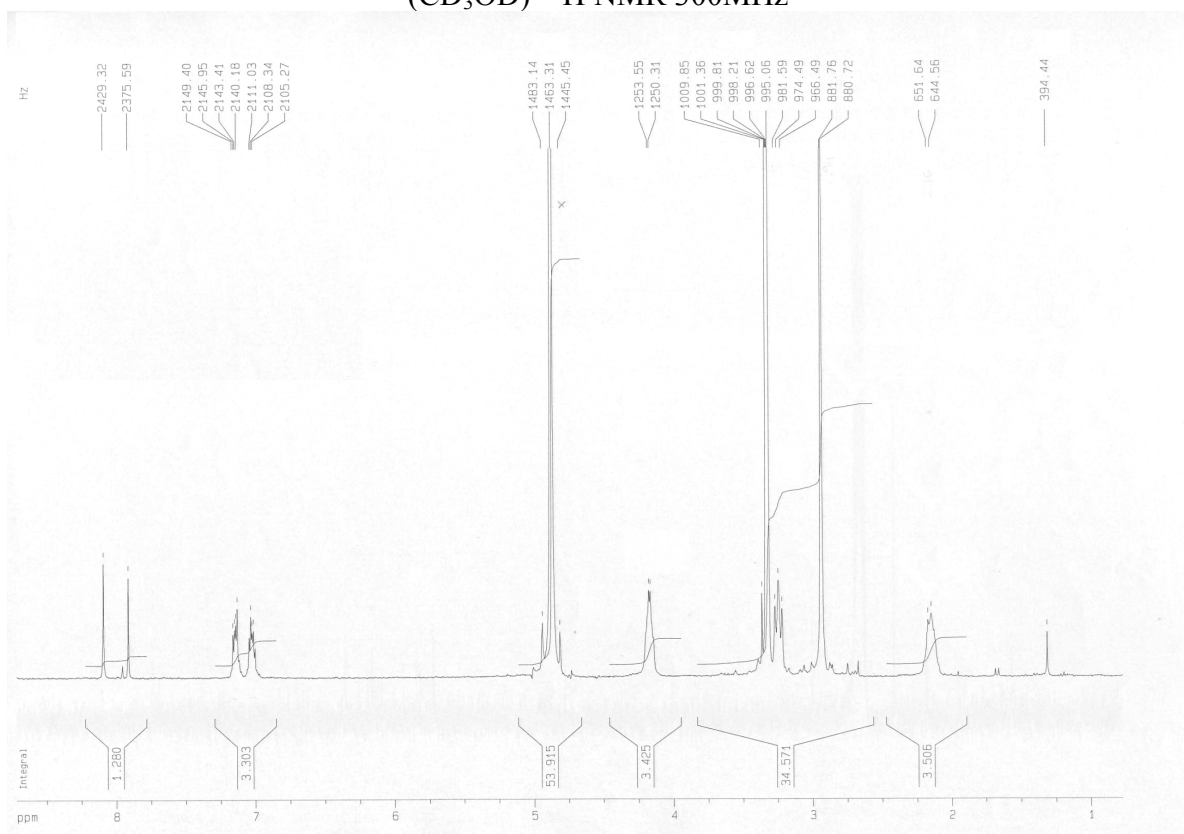
2·2HCl (CD₃OD) ¹H NMR 300MHz



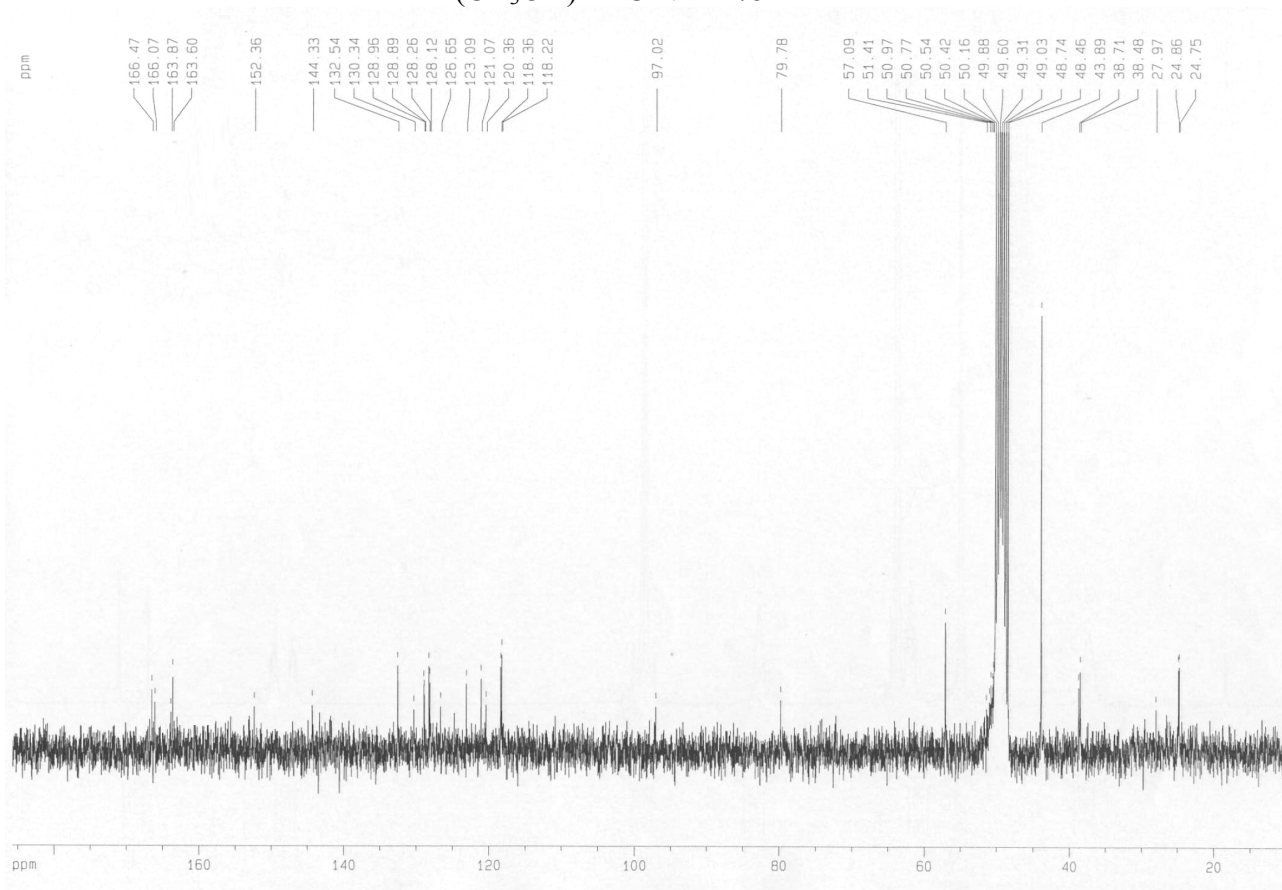
(CD₃OD) ¹³C NMR 75MHz



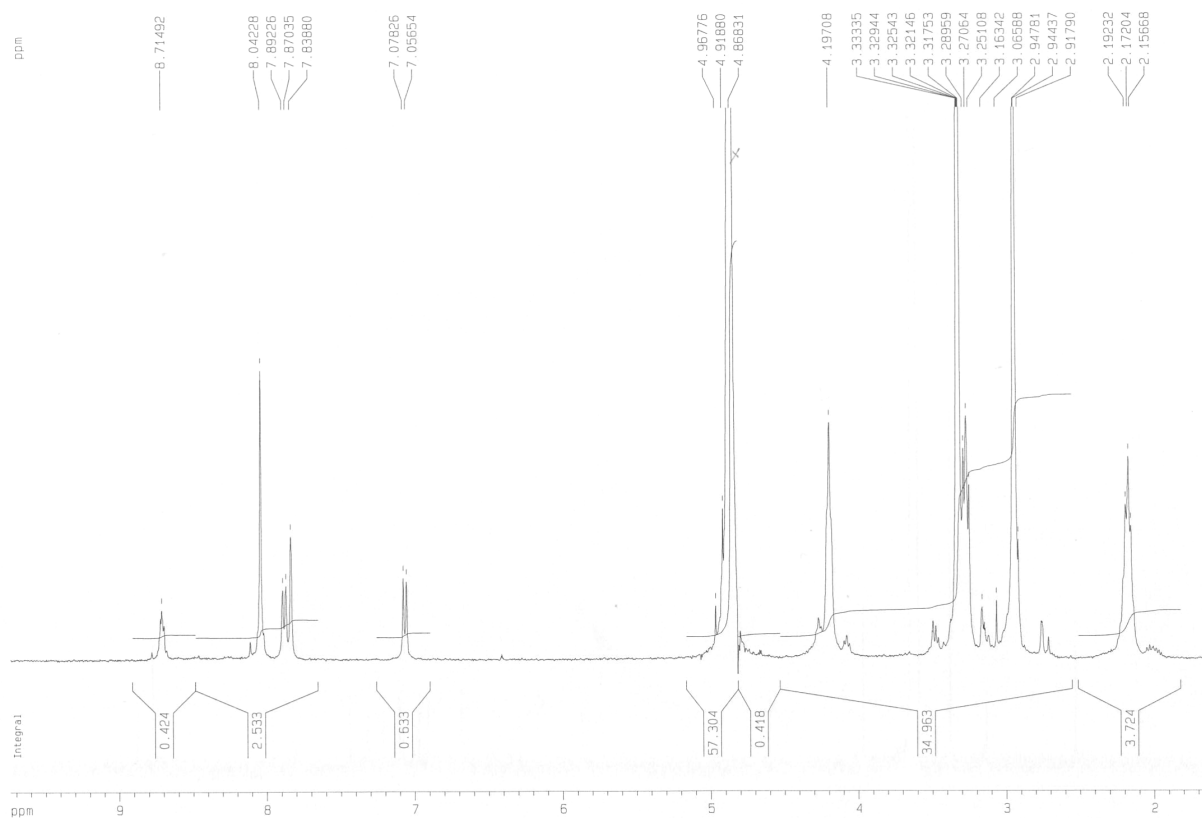
3·2HCl
(CD₃OD) ¹H NMR 300MHz



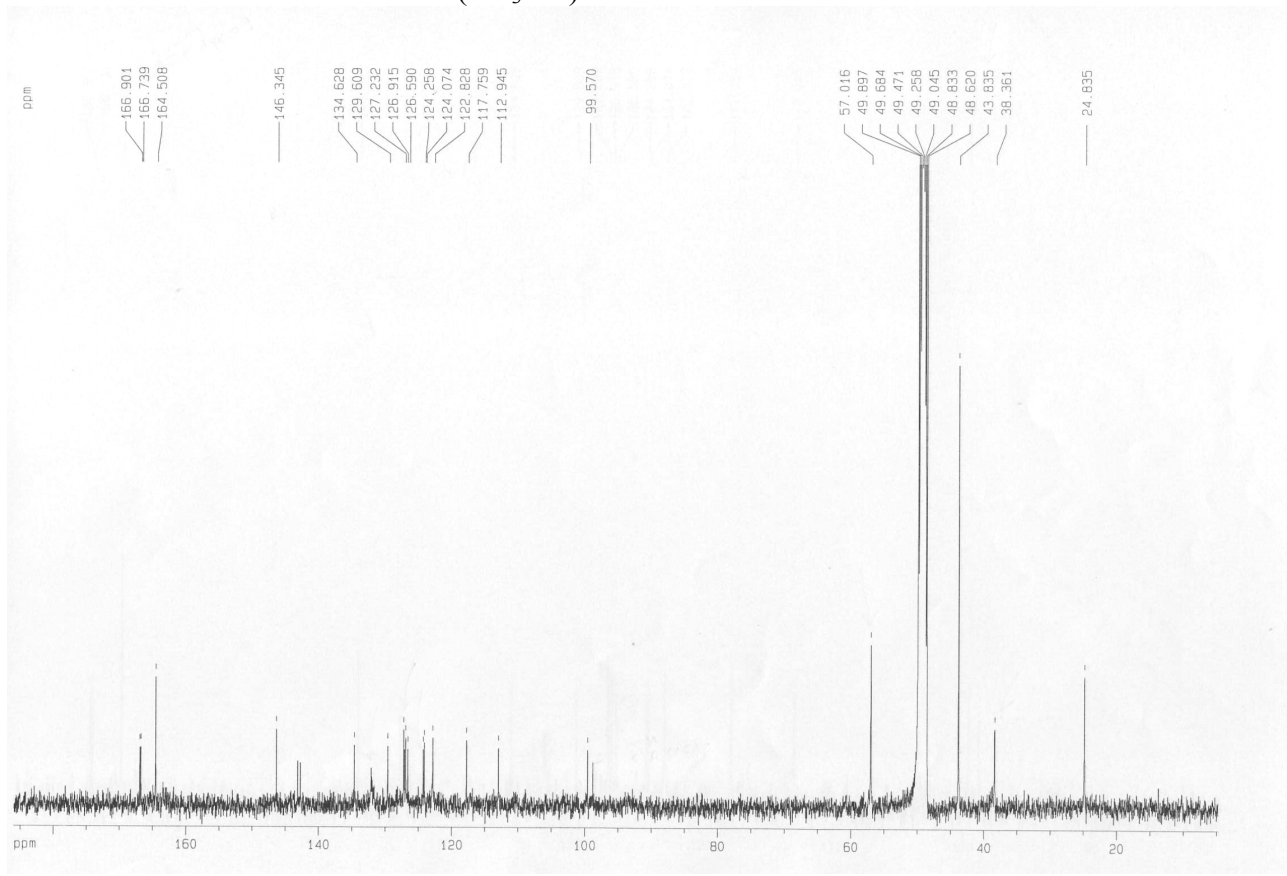
(CD₃OD) ¹³C NMR 75MHz



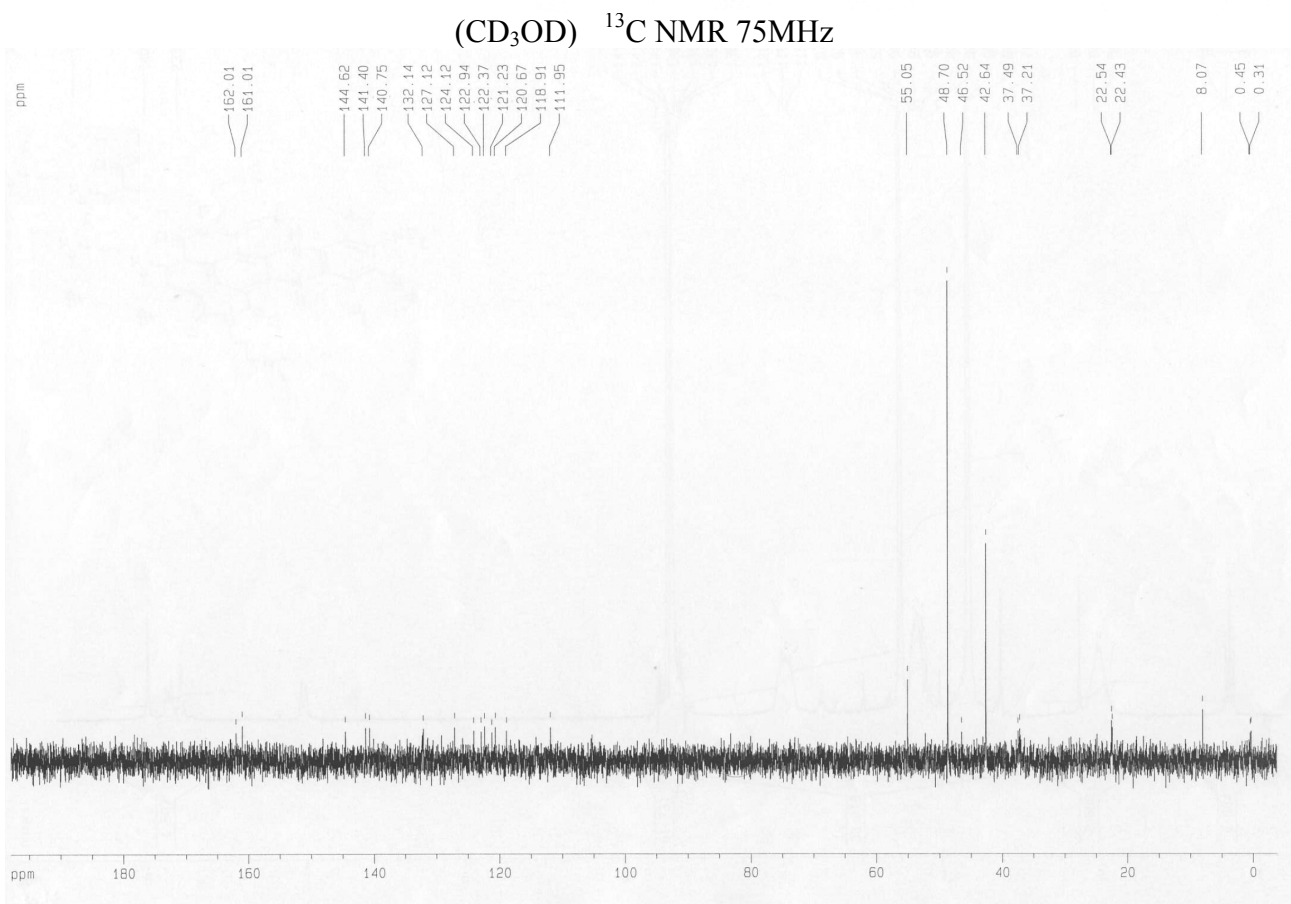
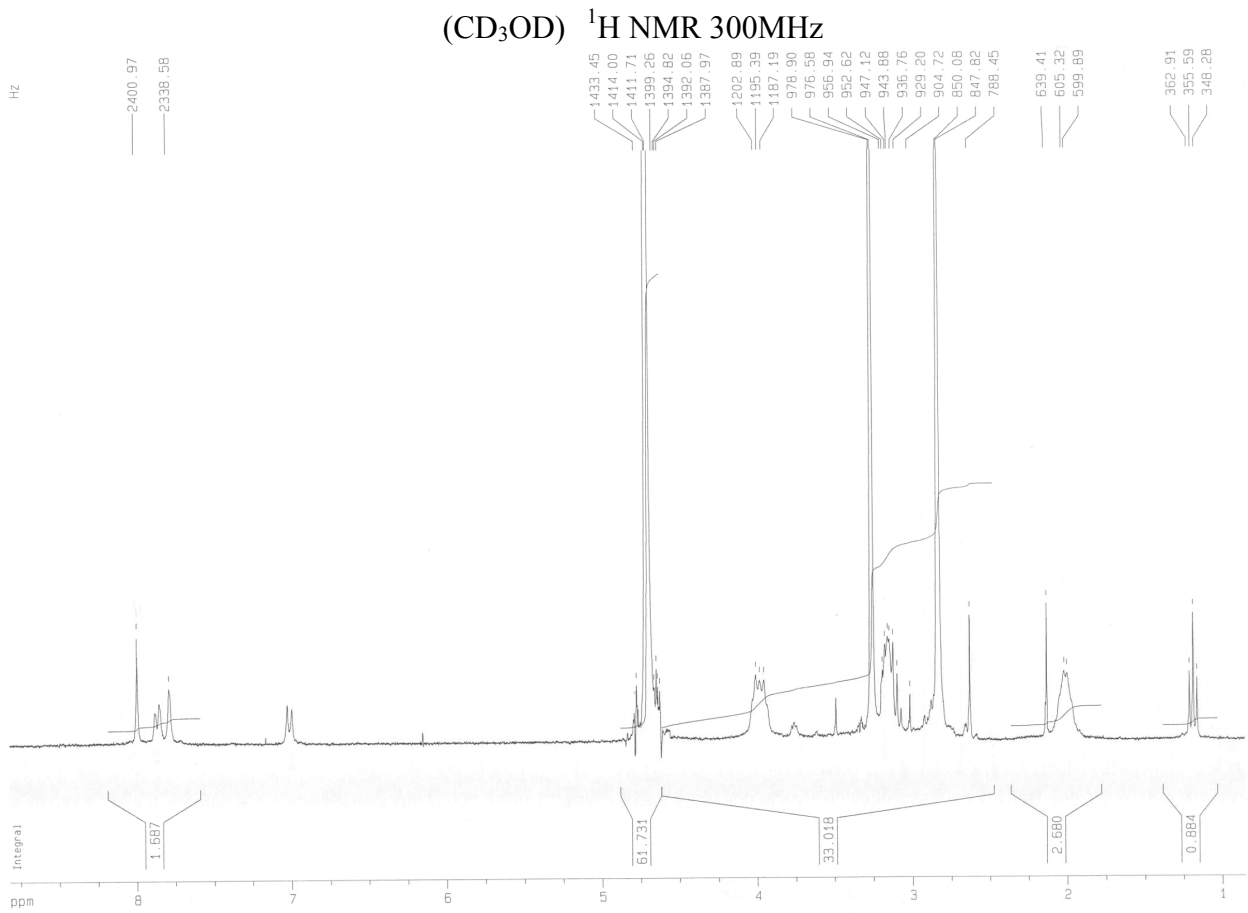
4·2HCl
(CD₃OD) ¹H NMR 300MHz



(CD₃OD) ¹³C NMR 75MHz

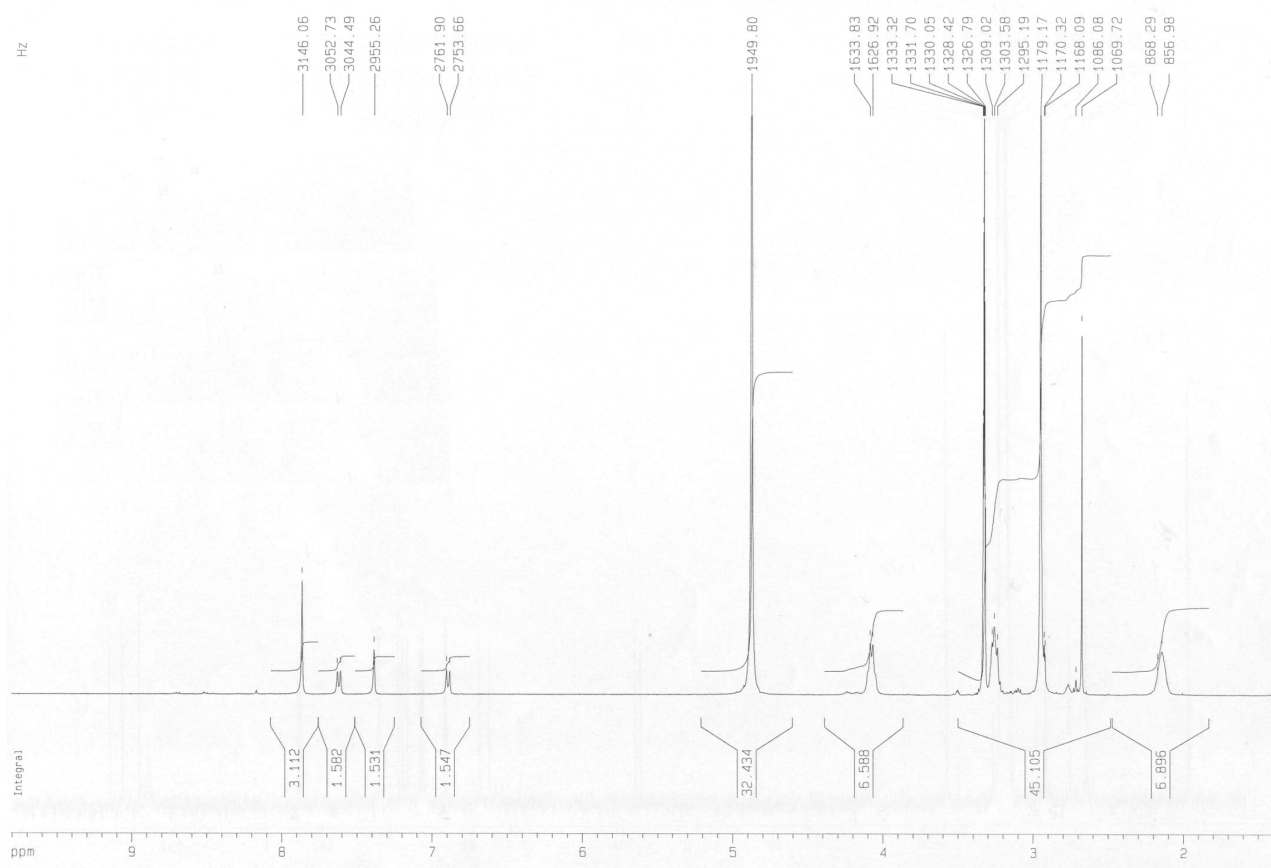


5·2HCl

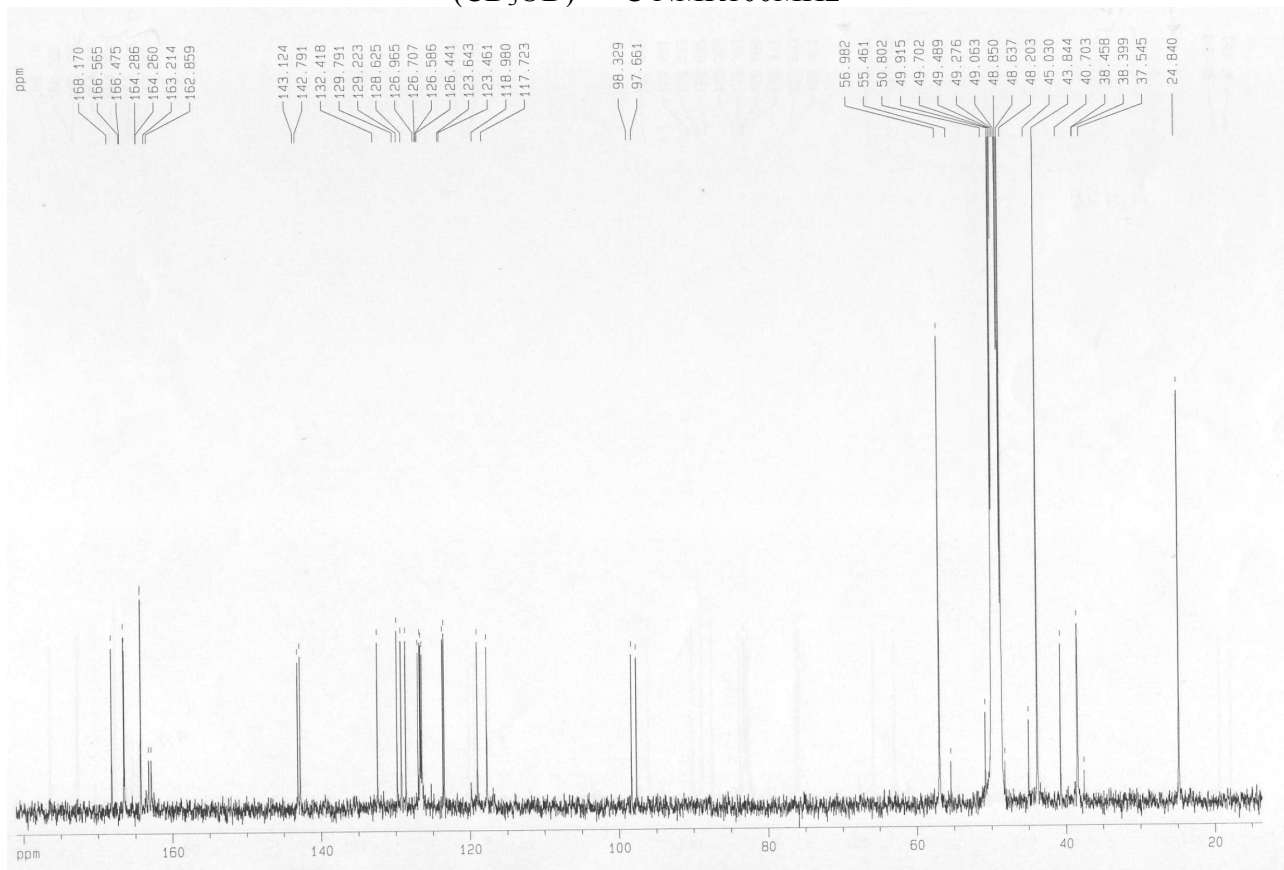


6·2HCl

(CD₃OD) ¹H NMR 400MHz

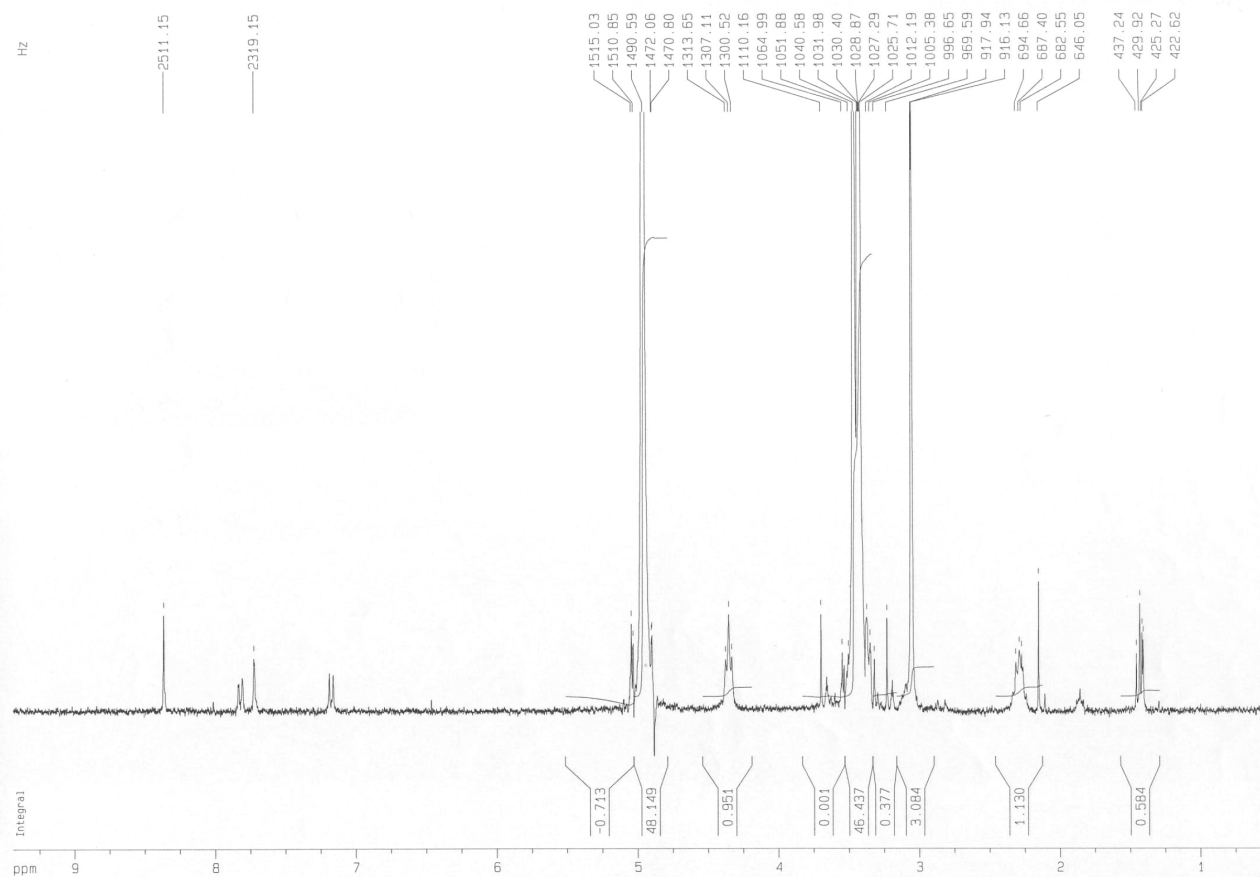


(CD₃OD) ¹³C NMR 100MHz

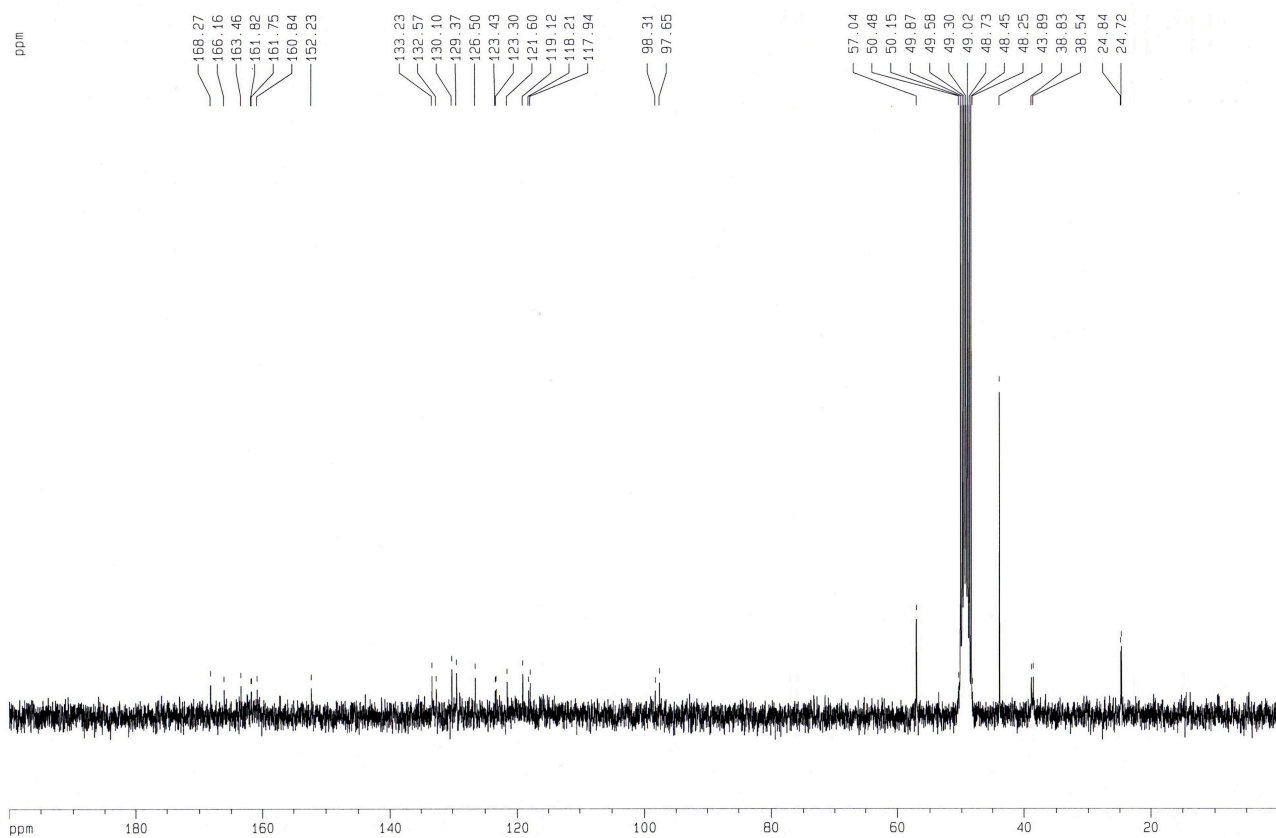


7·2HCl

(CD₃OD) ¹H NMR 300MHz

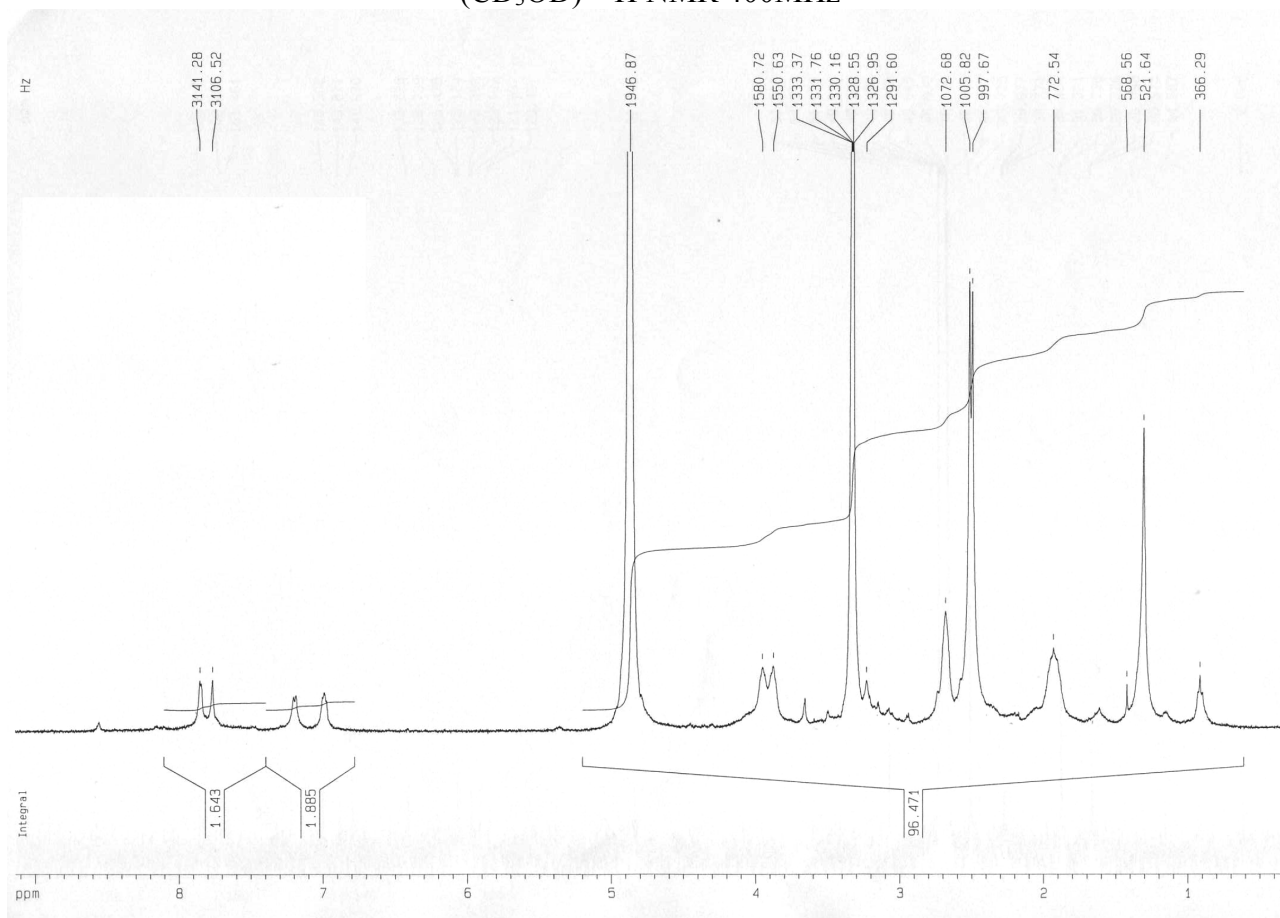


(CD₃OD) ¹³C NMR 75MHz

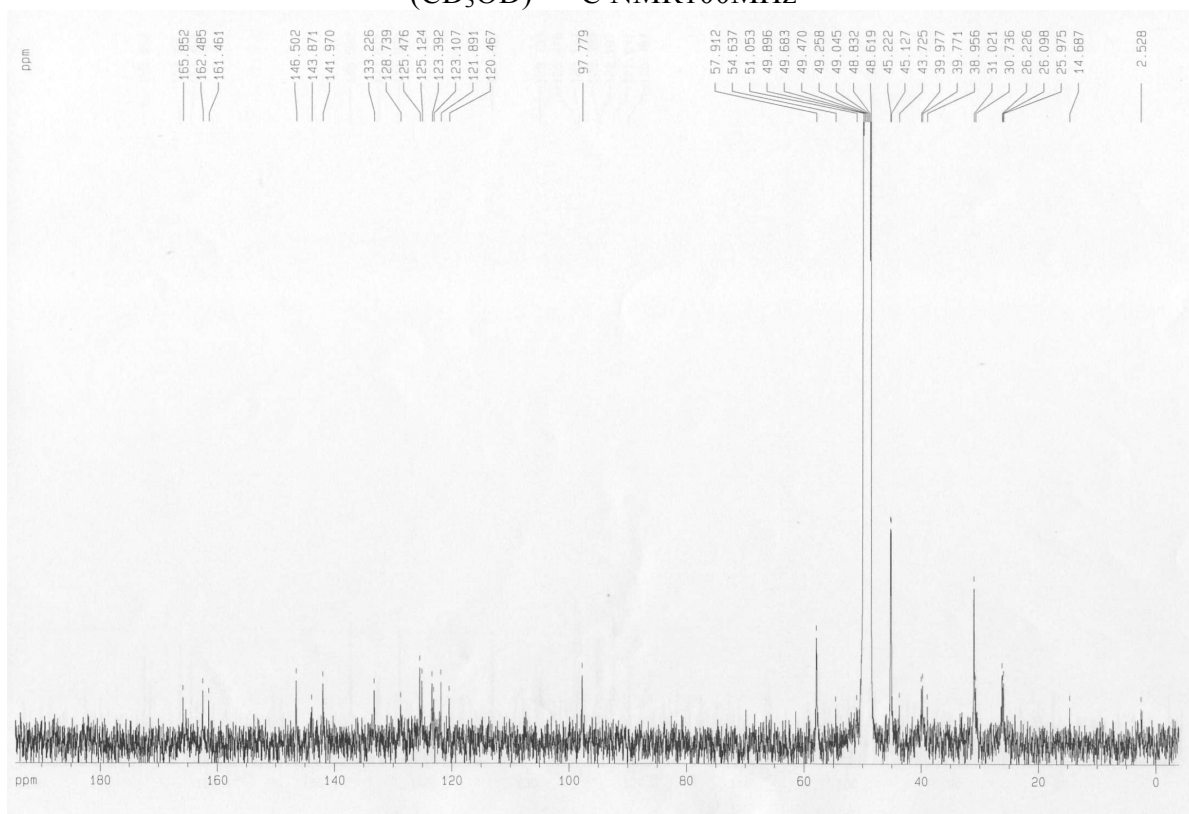


8-3HCl

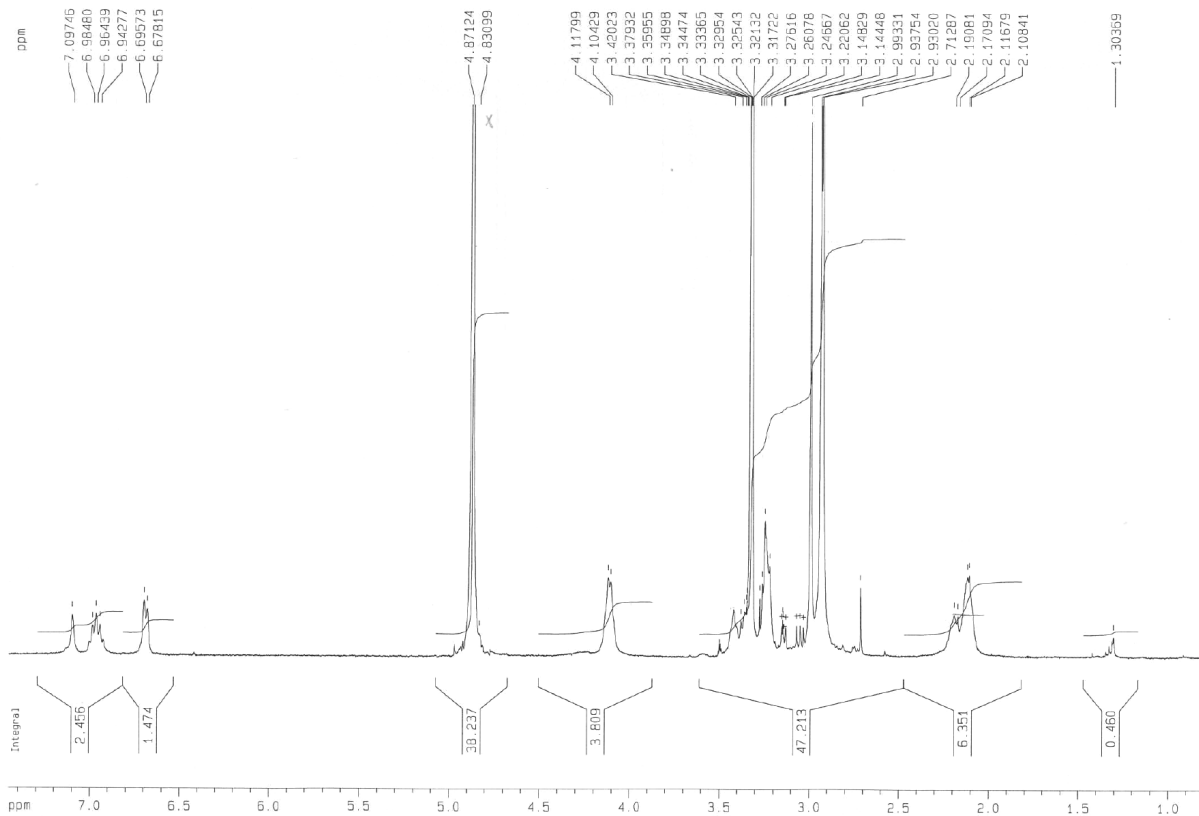
(CD₃OD) ¹H NMR 400MHz



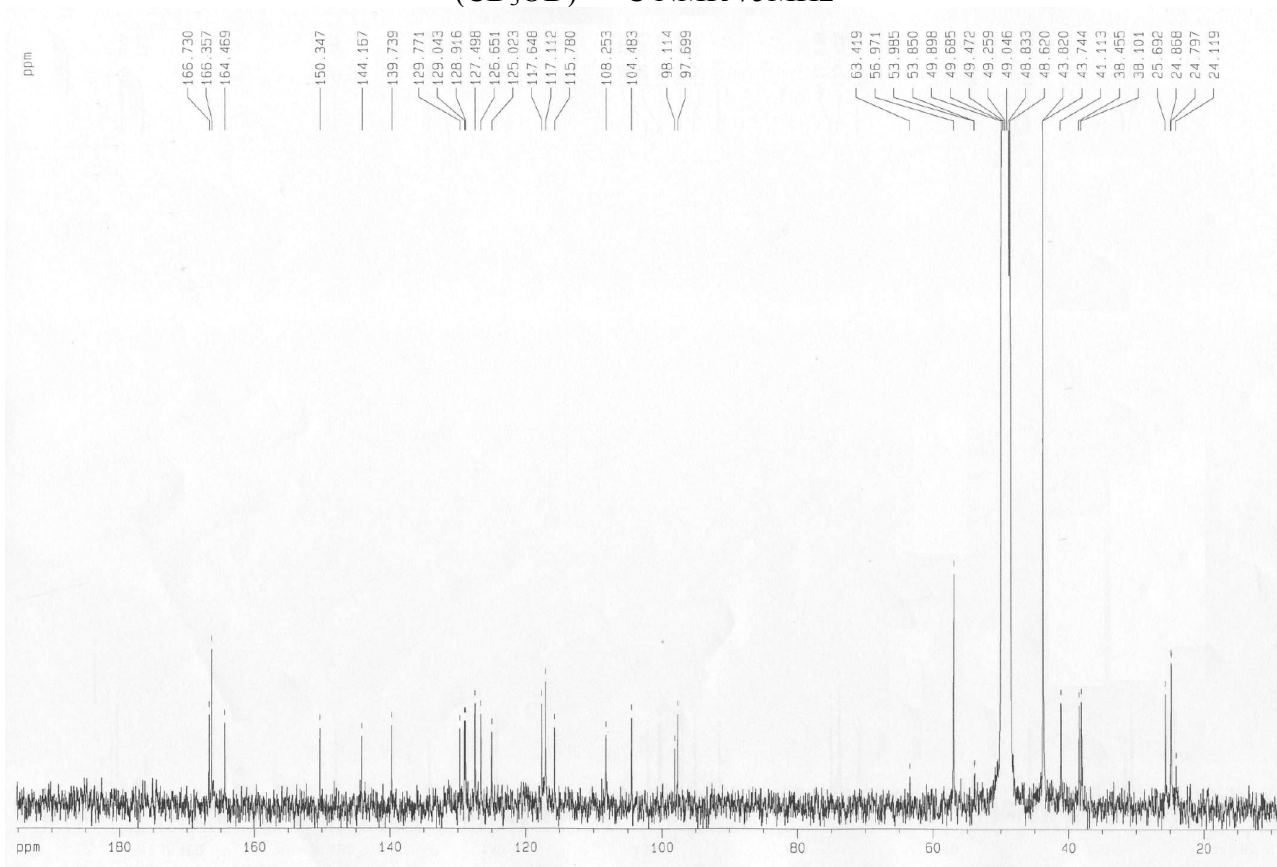
(CD₃OD) ¹³C NMR 100MHz



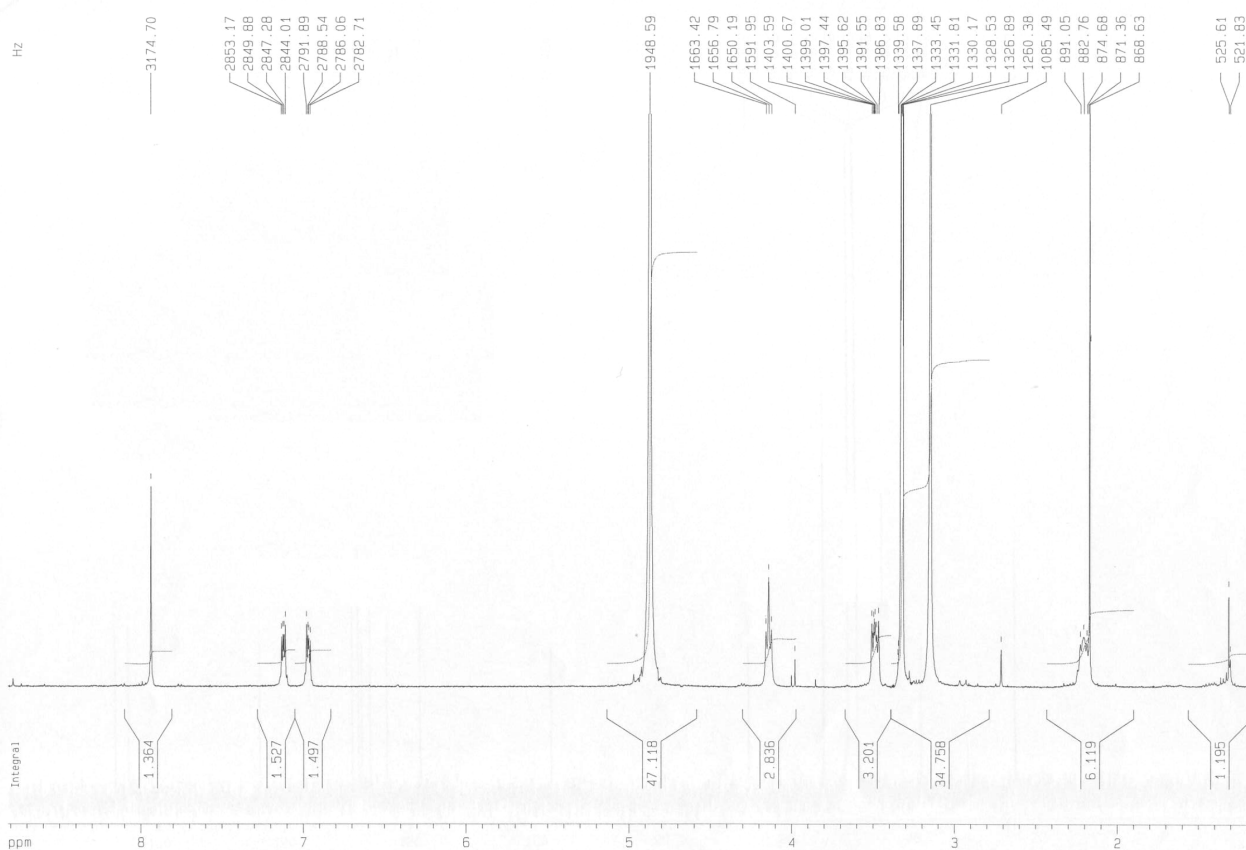
9-3HCl
(CD₃OD) ¹H NMR 300MHz



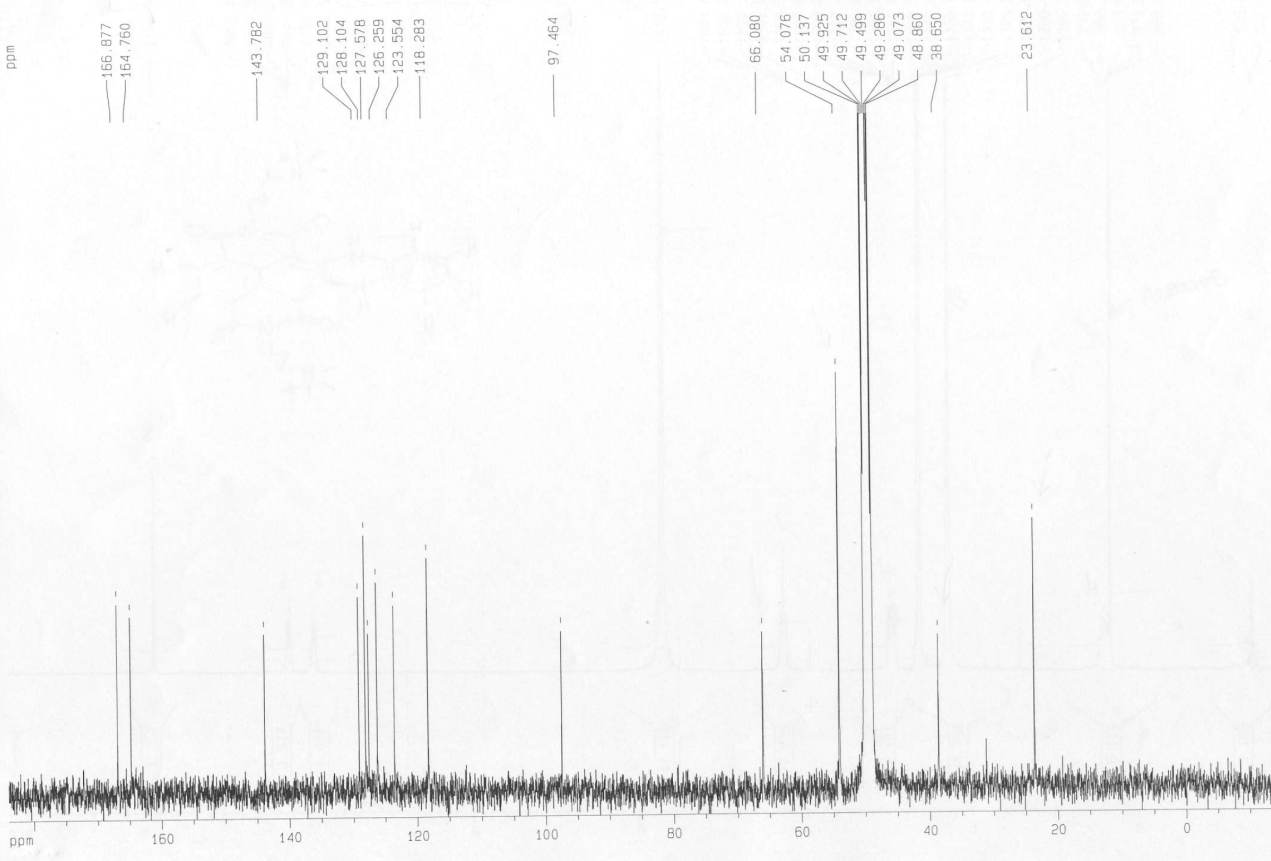
(CD₃OD) ¹³C NMR 75MHz



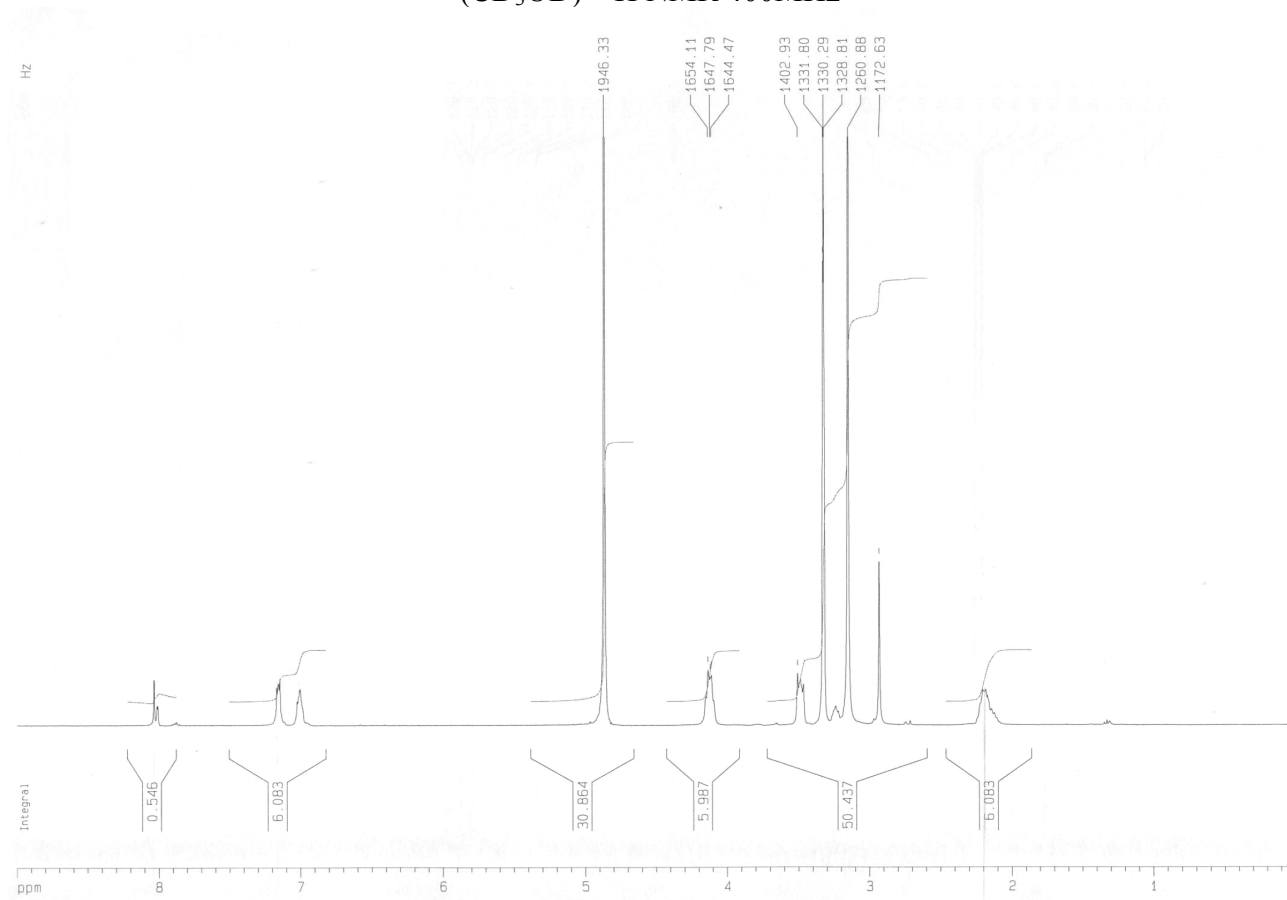
10
(CD₃OD) ¹H NMR 400MHz



(CD₃OD) ¹³C NMR 100MHz



11
(CD₃OD) ¹H NMR 400MHz



(CD₃OD) ¹³C NMR 100MHz

